Mesocosm approaches to the examination of benthic–pelagic coupling, with emphasis on turbulence

Elka T. Porter [1*], Jeffrey C. Cornwell [2]
[1]St. Mary's College of Maryland, St. Mary's City, Maryland, USA
[2]Horn Point Laboratory, University of Maryland Center for Environmental Science, Cambridge, Maryland, USA

Abstract

Benthic and pelagic processes are closely coupled in shallow-water estuarine and marine environments and in lakes yet benthic–pelagic coupling is difficult to simulate in mesocosms. Realistic water column (WC) and bottom turbulence often are not simultaneously mimicked in mesocosm experiments, leading to artifacts and omitting direct and indirect linkages and feedbacks between the sediment and the WC. The information on benthic–pelagic coupling mesocosm studies assembled illustrates the importance of realistic physics in mesocosms. Mesocosm approaches including both WC turbulence and bottom turbulence that are appropriately designed to resemble natural conditions can provide a deeper mechanistic understanding of feedback processes associated with biogeochemical, food web, and the habitat shifts necessary for models, and will help identify cause-and-effect relationships. Benthic–pelagic mesocosm experiments with realistic WC and bottom turbulence may fill the large gaps in our understanding of the responses of inorganic nutrient and organic matter fluxes between benthic habitats and the WC. Future applications of such benthic–pelagic coupling mesocosm studies are outlined.

In shallow water aquatic systems, including lacustrine (Evans 1994), estuarine and marine environments (Threlkeld 1994), the study of interactions between benthic and water column (WC) environments can be important for understanding sedimentological, biogeochemical, and biological processes. "benthic–pelagic coupling" (BPC), incorporates particle dynamics such as deposition and resuspension as well as the exchange of solutes and gases produced or consumed in association with organic matter mineralization (Porter et al. 2018a). BPC has been described by alternate terminology such as "habitat couplings," "bentho pelago," "bentho-pelagic," "pelago-benthic," "habitat couplings," and "benthic–pelagic relationships" (Schindler and Scheuerell 2002; Chatterjee et al. 2013). Processes at the sediment–water interface influence the dynamics of contaminants and nutrients, faunal abundance and composition, and water quality. Pelagic and benthic ecosystems have important linkages that are indirect and nonlinear (Wootton 2002; Krivtsov 2004; Porter et al. 2004a; Najjar et al. 2010) and thus difficult to assess. Mesocosm physical characteristics including temperature, light, depth, tank dimensions, and mixing are all important physical controls of BPC and subsequent effects on organisms, overall trophic status and interactions, and biogeochemical cycling.

Models for forecasting need a detailed mechanistic understanding of benthic–pelagic processes and feedbacks to supply good data for models (Testa et al. 2017). If we look at the benthos and at the WC separately, we miss many indirect links and feedbacks and may even be introducing artifacts. Thus, models need experimental data where both the benthos and the WC are represented realistically and appropriately coupled. Inclusion of BPC data with feedbacks and indirect links of biogeochemical processes and food webs into models can yield better predictive results. At present, the mechanistic understanding of benthic–pelagic processes and feedbacks is insufficient (Griffith et al. 2017; Testa et al. 2017). In addition, fluxes between the benthos and the WC may be poorly characterized, especially regarding processes associated with resuspension and biogeochemical cycling (Griffiths et al. 2017; Porter et al. 2022); flux measurements under in situ resuspension are generally unavailable.

The utility of the mesocosm approach lies in its ability to explore and test mechanisms (Benton et al. 2007) and identify

*Correspondence: etporter@smcm.edu

cause-and-effect relationships (Stewart et al. 2013). Physical forcing such as mixing in experimental ecosystems has been shown to be critically important in mesocosm studies and the quantification and reporting of mixing has been recommended (Sanford 1997; Peters and Redondo 1997; Sanford et al. 2009). Examples of mesocosms introduced in this review, their pros and cons as well as their function as pelagic, benthic, or benthic–pelagic system is provided in Table 1. This review is novel in its synthesis of benthic–pelagic coupling in mesocosms emphasizing turbulence, an overview of devices used over time, and insights of potentially misleading results if the benthos and the WC are studied disconnectedly. In addition, this review provides guidance for future scientific advancement, with one whole section dedicated to future applications.

Focus on the WC, OR on the bottom, but not both together

Typically, WC and benthic processes have been studied in a decoupled way, focusing either solely on WC processes or solely on benthic processes (Sanford 1997; Baustian et al. 2014), ignoring any feedbacks between the two. For example, Arnott et al. (2021) reviewed 20 years of phytoplankton mesocosm studies that used artificially generated turbulence and focused solely on the WC, and found that mixing in the WC was primarily produced by aeration, grid flow, Couette flow, and shaker setups. Interestingly, the number of mesocosm phytoplankton studies with turbulence has declined dramatically since ~ 2005 (Arnott et al. 2021). Testa et al. (2017) also found that estuarine mesocosm studies have declined by ~ half since 2004 and suggest a need to "resuscitate" experimental ecosystem research to help enhance a mechanistic understanding of estuarine processes needed for forecasting.

Compared to the turbulent range in natural environments, many mesocosm experiments overmix the WC (Arnott et al. 2021, Fig. 1, as has also been found by Peters and Redondo 1997, Fig. 2). As noted by Arnott et al. (2021), early studies that focused on the effect of turbulence on phytoplankton growth (e.g., White 1976; Pollingher and Zemel 1981; Savidge 1981) did not try to quantify turbulence in their phytoplankton studies. Mixing is often not measured (e.g., Striebel et al. 2013) although it is key for WC ecosystem processes (Peters and Redondo 1997; Sanford 1997; Sanford et al. 2009). A sediment bottom was also not deemed important, and the focus was solely on WC processes, disconnected from any reciprocal interactions and feedbacks between WC and bottom. Some marine and freshwater studies incorporate shape and size of the mesocosms into their experiments (Berg et al. 1999; Petersen et al. 2003; Spivak et al. 2011); however, complete physical dimensions are often not reported thus leading to implicit scaling, as identified in a literature review (Petersen et al. 1999).

Similarly, experiments have been carried out in benthic-boundary-layer devices with bottom turbulence, focusing on processes at the bottom and sediment erosion (Widdows et al. 2007), where the devices have a negligible WC (Table 1). For short, small scale erosion studies, for example, "EROMES" laboratory erosion chambers (Andersen 2001; Kalnejais et al. 2007; Wengrove et al. 2015, Joensuu et al. 2018) or "Gust microcosms" (Gust 1990); Gust and Mueller (1997) have been used. Microcosms have also been used by Tengberg et al. (2004) and Law et al. (2016). In addition, annular or linear stream flumes have been used ("Sea Carousel" Maa et al. 1993, 1998; Widdows et al. 1998; Widdows et al. 2007, 2008; Jones et al. 2015) to measure sediment erodibility.

Widdows et al. (2007), in an inter-comparison of five benthic-boundary-layer devices for erodibility of intertidal sediments, found different types of annular flumes were able to record significant differences in the erodibility of soft sediments. A cohesive strength meter (CSM) and EROMES laboratory erosion chambers were not very effective in measuring differences in erosion thresholds of soft estuarine sediments. To study the short-term interactions of water flow and contaminants, particle entrainment simulators have often been used (Tsai and Lick 1986; Latimer et al. 1999; Orlins and Gulliver 2003; Cantwell and Burgess 2004 and review therein).

Karle et al. (2007) developed a boxcosm system for ecological and/or ecotoxicological studies of sediment community function and structure with flow-through incubations, though benthic boundary-layer flow was not assessed. While bottom stress can be mimicked and sediments were included, the short water residence time precluded WC processes.

Reciprocal feedbacks from WC ecosystem processes cannot be incorporated in these experiments with benthic boundary-layer devices, and often experiments in benthic-boundary-layer devices are very short-term. Another design of a benthic boundary-layer device is the Tidal Dynamics WAVE flume (TiDyWAVE) that focuses on oscillatory flow velocities (de Smit et al. 2020). It can mimic peak oscillatory velocities between 0.09 and 0.32 m s^{-1}, which correspond to wave periods ranging from 4.0 to 3.5 s, respectively, and it can mimic sediment erodibility (de Smit et al. 2020, Table 1). When de Smit et al. (2020) compared oscillatory flow in the TiDyWAVE to natural waves they found that the TiDyWAVE did not realistically simulate WC processes such as particle aggregation/disaggregation. Thus, only benthic boundary-layer flow experiments, for example, erosion studies, are possible in the TiDyWAVE and there is also no benthic pelagic coupling component with its associated direct and indirect interactions and feedbacks between the benthos and a WC.

Meysick et al. (2022) used a 0.8 m long, 0.5 m wide, and 0.5 m high hydraulic wave flume to study the interactive effects between eelgrass, *Zostera marina*, and *Limecola balthica* (= *Macoma balthica*) and with *Cerastoderma edule*. While an increasing density of *M. balthica* has been found to increase

Table 1. Examples of mesocosms in the review, their pros and cons, and their function as pelagic (P), benthic (B), or benthic–pelagic (BP) systems.

Mesocosm	P, B, BP	Pros	Cons	References
Mesocosms	P	Attempts to study the effects of mixing on phytoplankton.	RMS turbulent velocity, energy dissipation rate and bottom shear stress not measured. Mixing with disc, air bubbles, airlift system, no mixing.	Striebel et al. (2013)
Benthic–pelagic Mesocosm	P	Sediment, WC.	Mixing and shear stress not measured. Artificially depositional environment affected biogeocheochemical variables.	Dimitriou et al. (2017)
Small isolated tank	P	Sediment, realistic WC mixing.	Light limited. Unrealistic low bottom shear stress, bottom and WC not well coupled.	Review by Arnott et al. (2021)
Large isolated tank, excessive WC mixing	P	Resuspension might be achieved by increasing the stir rate.	Energy dissipation rate is too high which can lead to altered particle aggregation/disaggregation, altered contact rates between copepods and their food particles. Bottom and WC not well coupled. Ecosystem effects.	Review by Arnott et al. (2021), Porter et al. (2010)
Large isolated tank, realistic WC mixing	P	Realistic WC turbulence can be achieved without overmixing the WC. Many phytoplankton studies have used these systems. Non resuspension.	Unrealistic low bottom shear stress, bottom and WC not well coupled. Distorted diffusive sublayer, distorted BP, mismatch artifacts, missed indirect links. Ecosystem effects.	Donaghay and Klos (1985), Porter et al. (2004a, 2010)
MEERC and MERL isolated tanks	P	Short term resuspension in MERL cosms, no mixing and shear stress measured. Realistic WC mixing in MEERC allows pelagic experiments. Sediment.	Unrealistic low bottom shear stress in MEERC tanks, bottom and WC not well coupled. Ecosystem effects.	
Traditional flumes	B	Bottom shear stress can be mimicked.	There is no deeper quiescent WC. No continuous sediment bottom.	Muschenheim et al. (1986), Nowell and Jumars (1987), Butman et al. (1994), Grizzle et al. (1994)
Annular flumes, particle entrainment simulator, EROMES, Gust microcosm	B	Bottom shear stress can be mimicked and sediments included.	No deeper quiescent WC. No indirect links and feedbacks.	Gust and Mueller (1997), Tengberg et al. (2004), Kalnejais et al. (2007), Tsai and Lick (1986), Orlins and Gulliver (2003), Maa et al. (1998), Widdows et al. (1998)
Tidal dynamics WAVE flume (TiDyWAVE)	B	Sediment erosion can be studied.	Limited to boundary-layer processes, no WC with WC processes.	de Smit et al. 2020
Large linked Mesocosm (annular flume + Mesocosm)	BP	Uses defined, uniform bottom shear stress levels below critical erosional shear stress, and realistic WC mixing. Includes sediment.	Connecting lines do not allow runs with high shear stress with resuspension. Particulates cannot reliably pass connecting lines. Complex to run.	Porter et al. (2004a,b)

(Continues)

Table 1. Continued

Mesocosm	P, B, BP	Pros	Cons	References
Small linked Mesocosm (Gust microcosm + Mesocosm)	BP	Uses defined, uniform shear stress levels below critical erosional shear stress, and realistic WC mixing. Includes sediment.	Light-limited. Connecting lines do not allow runs with high shear stress with resuspension. Particulates cannot reliably pass connecting lines complex to run.	Porter et al. (2004a,b)
Benthic WC simulator	BP	Measures both, bottom shear stress and WC RMS turbulent velocity.	It is small and cannot be used for ecosystem experiments. Energy dissipation rate not measured.	Kleeberg et al. (2013), Kleeberg and Herzog (2014)
STURM	BP	Measures both, bottom shear stress and WC turbulence. Includes resuspension without overmixing the WC. Replication. Realistic BPC, feedbacks, indirect effects.	Can only be used with muddy sediments. Presently does not accommodate epifaunal organisms.	Porter et al. (2018a,b, 2010, 2013, 2020a,b; 2022), Schneider et al. (2007), Kim et al. (2004, 2006)
Wave Mesocosms, wave flumes	BP	Realistic relevant regular and irregular wave conditions can be generated.	Typically, energy dissipation rate is not quantified as well as RMS turbulent velocity. However TKE and mean orbital velocity are often measured.	Blottière et al. (2017), Marin-Diaz et al. (2019), Infantes et al. (2021)

TKE = total kinetic energy.

sediment erodibility, as observed in annular flumes (Willows et al. 1998; Widdows et al. 2000) Meysick et al. (2022) found monospecific *M. balthica* reduced erosion by 25% and monospecific *C. edule* increased erosion by 40% under wave exposure in a hydraulic wave flume. Eelgrass by itself reduced bedload erosion rates by 25–50% (Meysick et al. (2022).

Observations suggested that the combination of eelgrass and *M. balthica* together had positive additive effects on sediment stabilization. Eelgrass and *C. edule* brought together made the destabilizing effect of *C. edule* disappear. However, there was no WC, and observations were focused on the benthic boundary-layer.

In shallow-water estuarine and marine environments (Threlkeld 1994) and in lakes (Evans 1994), the importance of coupled benthic and pelagic processes is accentuated. Observing the WC and the benthos separately, especially in shallow water environments with a high benthic to pelagic habitat ratio, likely leads to artifacts (Sanford 1997). Baustian et al. (2014) identified artifacts in observations of organism movement, such as in diel migrations and life cycles, as an important experimental limitation without WC and benthic coupling. Moreover, they outlined trophic interactions between the benthos and the WC such as in lakes, estuaries and marine systems, as another mechanism that connects the benthos and the WC and that can cause shifts in community structure if benthos and WC are not studied together (Baustian et al. 2014). A third mechanism that connects benthos and WC, identified by Baustian et al. (2014), is biogeochemical cycling. Resuspension and associated fluxes of organic material and porewater between benthos and WC can alter biogeochemical processes (Moriarty et al. 2017). Porter et al. (2010) found that regular tidal resuspension impacted ecosystem structure and function, often through indirect pathways and linkages. Nutrient and oxygen balances were controlled by benthic and WC biogeochemical processes, as mediated by biodeposit resuspension in Porter et al. (2022).

Solid experimental and observational data on benthic–pelagic coupling processes are needed as input for models (e.g., Moriarty et al. 2017, 2018, 2020) that quantity the feedbacks and ecosystem responses in forecasting. One model that incorporates benthic pelagic coupling is the hydrodynamic-sediment transport biogeochemical model (HydroBioSed, Moriarty et al. 2017, 2018, 2020). Vadeboncoeur et al. (2002) worked on adding the benthos to the WC in lake food webs models and argued that benthic and pelagic organisms are both important and benthic and pelagic habitats are closely coupled.

Mesocosm approaches with both realistic WC turbulence and bottom turbulence can provide data for a deeper mechanistic understanding of feedback processes associated with biogeochemical, food web, and habitat shifts to inform such models and will help identify cause-and-effect relationships.
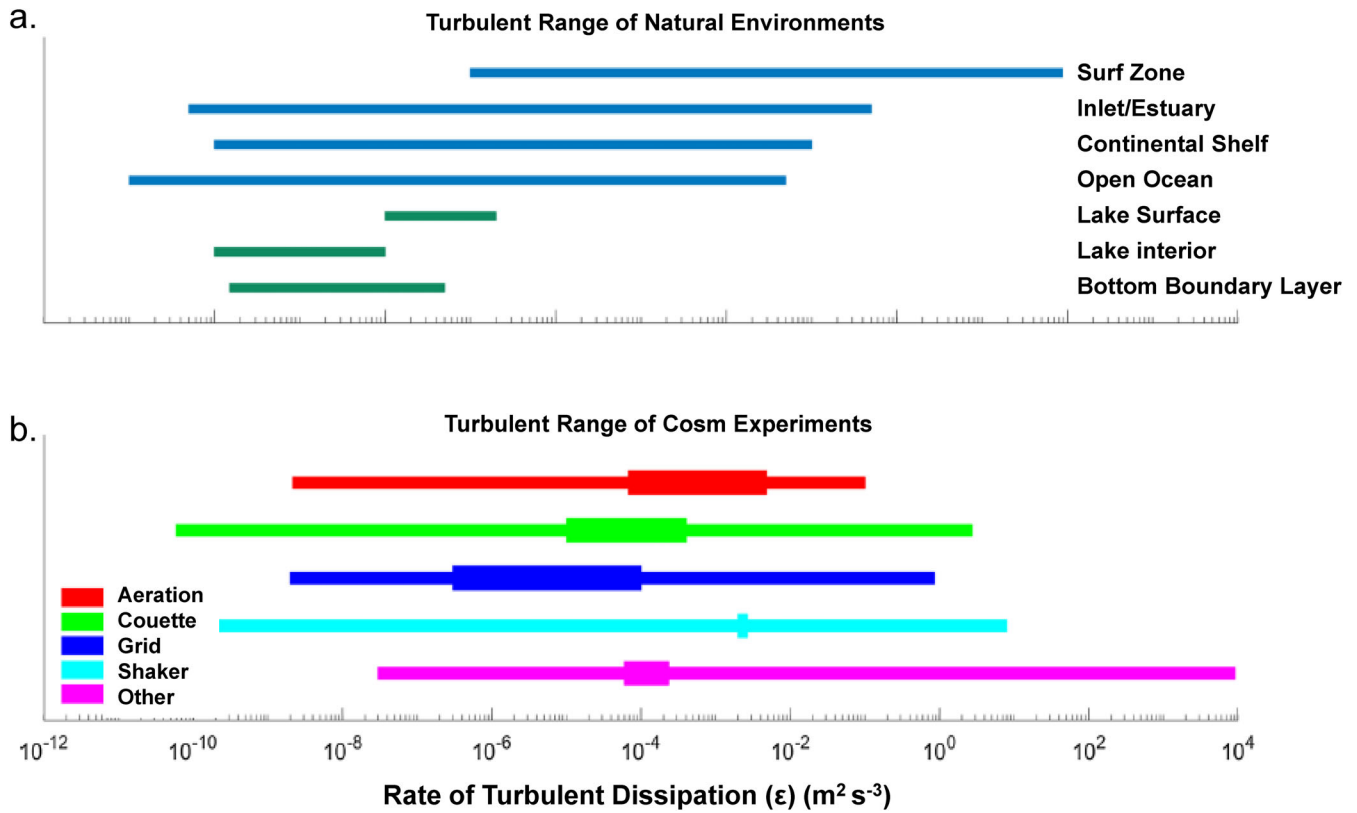
Fig. 1. (**a**) Turbulent range of natural environments as compared to (**b**) turbulent range of cosm experiments. From Arnott et al. 2021. http://creativecommons.org/licenses/by/4.0/.
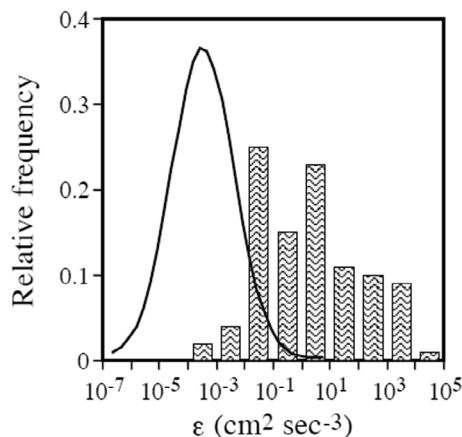

Fig. 2. Comparison of turbulence levels in the surface mixing layer of the ocean (line, after MacKenzie and Leggett 1993) to turbulence levels used in experiments with planktonic organisms. From Peters and Redondo 1997. Permission by Editorial CSIC.

Studies incorporate a sediment bottom in mesocosm experiments

A plankton tower mesocosm (von Bodungen et al. 1976) is one of the earliest designs to study interactions between the

WC and the sediments (Sharma et al. 2021, Fig. 3). The plankton tower mesocosm, built with four plastic bags with a steel framework to support the structure, had a pelagic WC and benthic ecosystem (Sharma et al. 2021, Fig. 3) but no mixing. The Marine Ecosystem Research Laboratory (MERL) in Rhode Island conducted a series of mesocosm experiments with sediments and investigated sediment-water interactions and ecotoxicology (Santschi 1985; Doering et al. 1986) while also considering mixing (Nixon et al. 1980) in their studies. Mesocosms with muddy sediments of the Multiscale Experimental Ecosystem Research Center (MEERC) created uniform WC mixing among mesocosms of different shapes and sizes, but bottom shear stress was artificially low (Crawford and Sanford 2001), which may lead to artifacts (Porter et al. 2010).

Realistic WC mixing, unrealistic u∗: Mismatch artifacts, missed indirect links

In natural shallow water environments, the ratio of RMS turbulent velocity and bottom shear velocity (u_*) is $\sim 1.44 \pm 0.08 : 1$ according to Baumert and Radach (1992), Gross and Nowell (1983), Gordon and Dohne (1973), and Bowden (1962) (Table 2). In the large coupled system (annular-flume + mesocosm WC) and small coupled system

(Gust microcosm + mesocosm WC; Porter et al. 2004*a*, Table 1), the ratio of root mean squared (RMS) turbulent velocity and bottom shear velocity was 1.6 (Porter et al. 2004*a*, Table 2). In large and small isolated MEERC tanks, the ratio was 7–7.5 : 1 (Porter et al. 2004*a*, Table 2) and bottom shear stress

was unrealistically low (Crawford and Sanford 2001; Porter et al. 2010, Table 2). Unrealistically, low shear stress in the tanks compared to large coupled systems with intermediate bottom shear stress led to microphytobenthos not being eroded with subsequent effects on the sediment biogeochemistry
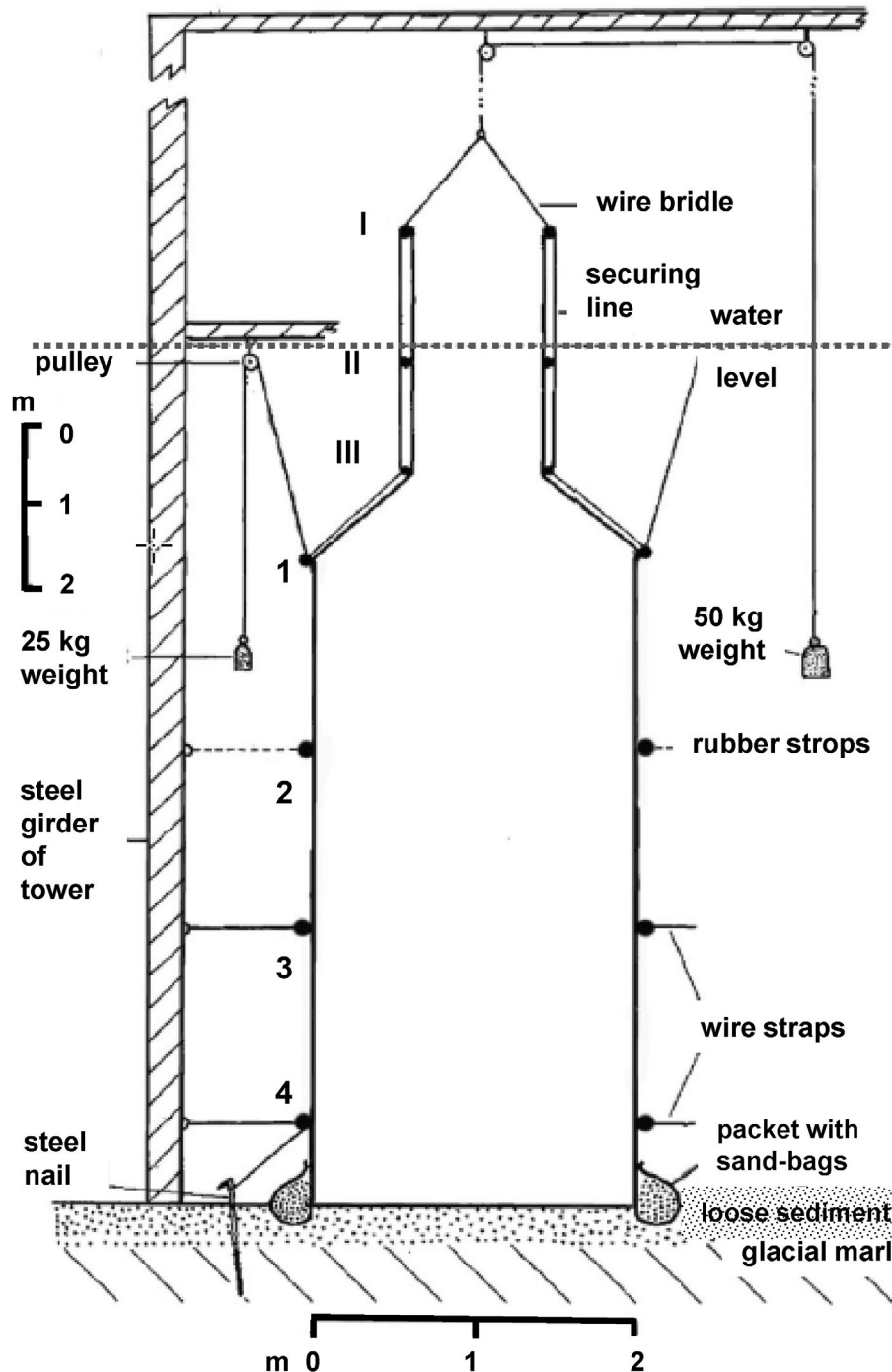

Fig. 3. Plankton tower mesocosm is one of the earliest designs to study interactions between the WC and the sediments (Von Bodungen et al. 1976). Plankton tower mesocosm consists of four plastic bags with steel framework for supporting the enclosures which have a pelagic WC and benthic Ecosystem. From Sharma et al. 2021. Permission by Springer Nature.

Table 2. Scaling relationships for water-column and benthic flow parameters derived from previous studies reporting RMS turbulent velocity (u_{RMS}) and shear velocity (u_*) in natural shallow-water environments, isolated tanks, coupled systems, and STURM.

| | | | | Where important | | | Pelagic–benthic | |
| | | | | Pelagic | | Benthic | | |
Observations	Location	Instrument	Depth (m)	Pelagic Energy dissipation rate ϵ (cm^2 s^{-1})	RMS turbulent velocity u_{RMS} (cm s^{-1})	Bottom shear velocity u_* (SD) (cm s^{-1})	Scaling relationship $u_{RMS} : u_*$	References
Model			5.1		4.3	3	1.49	Baumert and Radach (1992)
Field	Skagit Bay, WA	Ducted current meters	16		4.1	2.82	1.5	Gross and Nowell (1983)
Field	Choptank River, MD (estuary)	Pivoted vane	7.5		3.42	2.51	1.41	Gordon and Dohne (1973)
Field	Off Anglesey, North Wales	Electromagnetic current meter	12 to 22		4.85	3.6	1.34	Bowden (1962)
Large isolated tank	Mesocosm	ADV, shear stress sensors	1	0.02	0.95	0.127 (± 0.021)	7.5	Crawford and Sanford (2001), Porter et al. (2004a)
Small isolated tank	Mesocosm	ADV, shear stress sensors	1	0.03	0.99	0.141 (± 0.017)	7	Crawford and Sanford (2001), Porter et al. (2004a)
Large linked Mesocosm	Annular flume–Mesocosm	ADV, shear stress sensors	1	0.02	0.75	0.481 (± 0.234)	1.6	Porter et al. (2004a)
Small linked mesocosm	Gust microcosm–Mesocosm	ADV, shear stress sensors	1	0.03	0.94	0.588 (± 0.01)	1.6	Porter et al. (2004a)
STURM tank	Resuspension Mesocosm	ADV, shear stress sensors	1	0.003–2.65	0.57–4.52	0.087–1.688[a]	0.25–1.05[b]	Porter et al. (2018)

ADV, acoustic doppler velocimeter.
$u_{RMS} : u_*$.
Field 1.49.
Field 1.5.
Field 1.41.
Field 1.34.
Ave **1.44.**
SD **0.08.**
[a]Instantaneous spikes in shear velocity.
[b]Ratio of RMS turbulent velocity to spikes in shear velocity.

(Porter et al. 2004*a*,*b*). In tanks contrasting high bottom shear stress vs. low bottom shear stress but similar RMS turbulent velocity and energy dissipation rates, no sediments were resuspended in the nonresuspension systems (Porter et al. 2010). Resuspension of sediments in the resuspension systems led to less light in the ecosystem, but nutrient release from resuspended particles stimulated phytoplankton growth despite low light (Porter et al. 2010). In both cases, direct and indirect interactions were missed due to unrealistically low bottom shear stress, which artificially affected the feedback responses (Fig. 4).

High u∗, unrealistically high water-column mixing, artifacts

Changing nonresuspension mesocosms with uniform low bottom shear stress into resuspension tanks can be made by greatly increasing their stir rate. However, doing so will substantially overmix the WC and the energy dissipation rate will be artificially excessive. Particle aggregation and disaggregation (Hill et al. 1992; Riebesell and Wolf Gadrow 1992) and plankton contact rates and interactions (Rothschild and Osborn 1988; MacKenzie et al. 1994; Kiørboe 1997) are altered, affecting overall ecosystem processes.

Experimental induction of resuspension has utilized various methods, usually without measuring WC turbulence levels and bottom shear stress. For example, Kang (2013) and He et al. (2015) used submersible pumps, running continuously, to produce resuspension over 35–63 d. Ståhlberg et al. (2006) and Da-Peng and Yong (2010) resuspended sediment by shaking small incubation bottles and Acquavita et al. (2012) produced resuspension by using a horizontal shaker for 10 min at 130–150 cycles min^{-1}. Sutherland (2006) designed a mixing apparatus with paddles and bubbling of compressed air to maintain 7 d of turbidity in 38 L aquariums. Typically, mesocosm experiments are conducted in single isolated tanks or large bags with low bottom shear stress
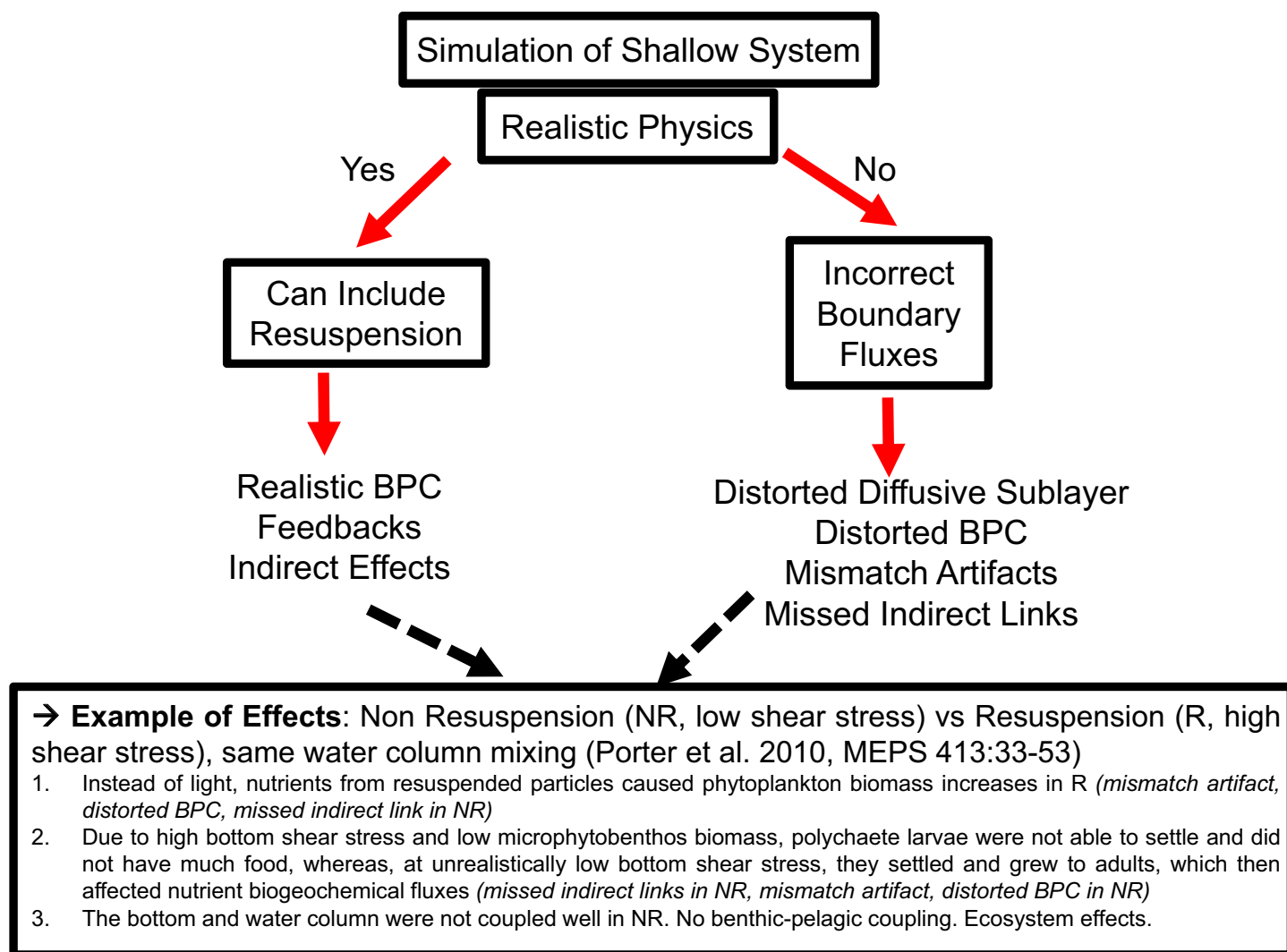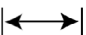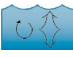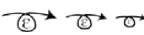

Fig. 4. Consequences of unrealistic mixing in experimental ecosystems. BPC = benthic–pelagic coupling.

Table 3. This table shows some of the turbulence scales that are important to consider when designing mixing for an experimental ecosystem.

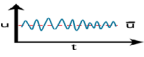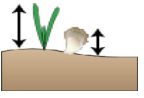|	Parameter	Name	Description	Typical values in the field
	Re	Reynolds number	Ratio of inertial to viscous forces (velocity scale × length scale/viscosity)	10^0 to 10^4 dimensionless, depends on definition
	u_{RMS}	RMS turbulence intensity	Characteristic turbulent (fluctuating) velocity in the WC	10^{-3} to 10^{-1} m s^{-1}
	l	Integral length scale	Size of the large eddies	Distance to the nearest boundary, or 10^{-2} to 10^{-1} m in the stratified interior
	K_Z	Vertical eddy diffusivity	Diffusion coefficient representing enhanced vertical mixing due to turbulence	10^{-6} m^2 s^{-1} in the stratified interior to 10^{-1} m^2 s^{-1} in an energetic bottom boundary layer
	T_m	Mixing time	Time to homogenize a tracer injected at a point	Minutes to days, depending on the size of the region of interest and the turbulent diffusivity
	ε	Turbulent energy dissipation rate[a]	Rate of destruction of turbulent energy by viscosity and shear	10^{-7} W m^{-3} in the stratified interior of the open ocean to 10^{-1} W m^{-3} in the surface layer under breaking waves
	η_k	Kolmogorov microscale	Approximate size of the smallest turbulent eddy	10^{-3} to 10^{-1} m for the range of ε
	$\overline{U}$	Mean flow speed	Time averaged flow speed	10^{-3} to 100 m s^{-1}
	u_*	Shear velocity[b]	Is $(t/p)^{1/2}$, where τ is bottom shear stress and ρ is water density; characteristic velocity scale in boundary layers	10^{-3} to 10^{-1} m s^{-1}
	K_b	Bottom roughness	Effective height of organisms or bedforms on the bottom	10^{-4} to 10^{-1} m
	δ_D	Diffusive boundary layer thickness	Thickness of layer that controls sediment-water fluxes	10^{-3} to 10^{-5} m

Additional guidance may be found in Sanford 1997. From Sanford et al. 2009. Permission by Springer Nature. Elka T. Porter is a coauthor on this book chapter. Permission by Springer Nature granted 15 August 2023 bookpermissions@springernature.com.
Bottom shear stress $\tau_b[\text{Pa}]\tau_b = \frac{u_*^2\rho}{10}$.
[a]Conversion of ε units: 100 mm^2 s^{-3} = 1 cm^2 s^{-3} = 1 erg g^{-1} s^{-1} = 10^{-1} W m^{-3} = 10^{-4} W kg^{-1} = 10^{-4} m^2 s^{-3}.
[b]Bottom shear stress: Fluid shear force per unit bottom area.

without any resuspension. Oviatt et al. (1981) and Sloth et al. (1996) successfully induced resuspension in the MERL mesocosms, but their resuspension event was short-lived. They did not measure WC turbulence or bottom shear stress.

Combined WC mixing and BBL-flow: Key for BPC studies/mixing measurements to include

In a study coupling a WC of a mesocosm with an annular flume or Gust microcosm bottom with muddy sediment, Porter et al. (2004a) first found that combined water-column mixing and benthic boundary-layer (BBL) flow are key for realistic benthic–pelagic coupling studies. Sanford (1997), Peters and Redondo (1997), Sanford et al. (2009; Tables 3–5), define and outline how to measure these important mixing

parameters when designing experimental ecosystems so that they fall in a realistic range. Critical WC turbulence parameters in mesocosm studies are the RMS turbulent velocity (u_{RMS}), the energy dissipation rate (ε) (Sanford 1997) and the ratio of RMS turbulent velocity and shear velocity (Porter et al. 2004a). For bottom turbulence, the bottom shear stress (fluid shear force per unit bottom area) should be determined, however, bottom shear stress is unrealistically low in traditional isolated mesocosms that have realistic WC turbulence levels (Crawford and Sanford 2001; Porter et al. 2010; Table 2).

One of the most important parameters of benthic turbulence in benthic boundary layers, related to erosion, entrainment, and sediment transport can be quantified as shear (or "friction") velocity u$_*$ (cm s^{-1}), a characteristic velocity scale in boundary layers (Gust 1988; Sanford et al. 2009). Benthic

Table 4. Important turbulent mixing relationships for key parameters in experimental coastal ecosystems.

Relationship	Comments	Where important
$u_{RMS} = \sqrt{\frac{1}{3}\left(u'^2 + v'^2 + w'^2\right)}$	where u', v', w' are the variable velocity components in the x, y, and z directions	Pelagic
$\varepsilon \approx \frac{u_{RMS}^3}{l}$	Integral length scale, l, is difficult to match between nature and experimental ecosystems	Pelagic
$K_Z \approx u_{RMS} * l \approx \varepsilon^{\frac{1}{3}} * l^{\frac{4}{3}}$	Turbulent diffusion controls mixing in WC and is difficult to match to nature because of l	Pelagic
$\eta_k = 2\pi\left(\frac{\nu^3}{\varepsilon}\right)^{\frac{1}{4}}$	ν = kinematic viscosity	Pelagic
$T_m = \frac{h^2}{2 * KZ}$	Often not as critical to match exactly if well mixed h is total depth or width	Pelagic
$u_* = \sqrt{C_D * \overline{U}}$	C_D is the hydraulic drag coefficient; depends on k_b and $\overline{U}$	Benthic
$\delta_D = \frac{10\nu}{u_*} * \left(\frac{D}{\nu}\right)^{\frac{1}{3}}$	D is the molecular diffusivity (note dependence on u_*)	Benthic

From Sanford et al. 2009. Elka T. Porter is a coauthor on this book chapter. Permission by Springer Nature granted 15 August 2023 book-permissions@springernature.com.

shear velocity is generated by velocities in the WC that may include steady flows, transients, waves (Terray et al. 1996), or stirring such as in the STURM tanks (Porter et al. 2018a,b). In most natural environments the shear velocity is created by wall-bounded shear flow. Tides affect bottom shear stress (Sanford et al. 1991) as do waves (Grant and Madsen 1979, 1982; Christie et al. 1999; Houwing 2000; Guillen et al. 2002). Moreover, wave-current interactions (Grant and Madsen 1982) such as storm events have the ability to mediate bottom shear stress. Shear velocity is calculated as

$$u_* = \sqrt{\frac{\tau_b}{\rho}} \tag{1}$$

where τ_b is bottom shear stress (dynes cm^{-2}) and ρ is the density of water (g cm^{-3}). Shear stress in units of dynes cm^{-2} multiplied by 0.1 equals shear stress in Pascal (Pa), the unit most commonly used. If, Eq. 1 is formulated differently, bottom shear stress [Pa] is calculated as

$$\tau_b = \frac{u_*^2 \rho}{10} \tag{2}$$

Table 5. Additional important turbulent mixing relationships.

Relationship	Comments	Where important
$U_{rms} = \sqrt{\frac{1}{N}\sum_{i=1}^{n}\left(ui^2\right)}$	Mean orbital velocity where u is the horizontal flow velocity during n measurement points.	Pelagic
$TKE = \frac{3}{2} u_{RMS}^2$	Total kinetic energy characteristic turbulent (fluctuating) velocity in the WC, related to RMS turbulent velocity (u_{RMS}).	Pelagic

Shear velocity ranges from 0.1 to 1 cm s^{-1} on the continental shelf and in microtidal estuarine benthic boundary layers (Grant et al. 1984; Sanford and Halka 1993; Gross et al. 1994). Shear velocity ranges from 1 to 10 cm s^{-1} in macrotidal estuarine benthic boundary-layers (Wright et al. 1992; Johnson et al. 1994). Shear velocity/stress at the bottom of mesocosms can be measured directly using hot-film anemometry (Gust 1988; Crawford and Sanford 2001; Porter et al. 2018a).

The most important variables for quantifying WC turbulence are root mean square RMS turbulent velocity u_{RMS} and turbulent energy dissipation rate ε (Peters and Redondo 1997; Sanford 1997; Sanford et al. 2009). RMS turbulent velocity is a characteristic turbulent (fluctuating) velocity in boundary layer flows and can be determined as defined in Tennekes and Lumley (1972):

$$u_{RMS} = \sqrt{\frac{1}{3}\left(<u^2> + <v^2> + <w^2>\right)} \tag{3}$$

where $<u^2>$, $<v^2>$, and $<w^2>$ are the variances of their respective velocity components. To determine the energy dissipation rate in mesocosm experiments, mean flow speed and RMS turbulent velocity must be determined, as they are necessary elements for the equation for energy dissipation rate.

Mean flow speed at each location in the mesocosm can be calculated as:

$$U_{Mean,tot} = \sqrt{U^2 + V^2 + W^2} \tag{4}$$

where U, V, and W are the mean flow velocities over the measurement interval, the W direction is vertical, and U and V are parallel to the water surface and orthogonal to each other. Energy dissipation rates can be determined following Gross et al. (1994), Terray et al. (1996), and Sanford (1997) as:

$$\varepsilon = \frac{2\pi}{[U_{Mean,tot}]or[u_{RMS}]} 1.9 \left[\frac{E(f)f^{\frac{5}{3}}}{2}\right]^{\frac{3}{2}} \tag{5}$$

where $E(f)$ is the measured turbulence spectrum over the inertial subrange. The ratio of mean flow speed (4) and RMS turbulent velocity (3) determines whether $U_{Mean,tot}$ or u_{RMS} is used in the denominator (left side) of Eq. 5 to determine energy dissipation rate (Sanford 1997). For mean flow speeds larger than the RMS turbulent velocity, $U_{Mean,tot}$ (Eq. 4) is used in the denominator to determine energy dissipation rate. For RMS turbulent velocity larger than the mean flow speed, u_{RMS} (Eq. 3) is used in the denominator. In addition, if the highest flow is not in the W (vertical) direction, the constant of 1.9 is used (Sanford 1997).

It is extremely difficult to simultaneously produce high near-bottom RMS turbulent velocities and appropriately low WC energy dissipation rates in the same experimental ecosystem because these parameters do not scale linearly together. RMS turbulent velocity and energy dissipation rate are related non-linearly as:

$$\varepsilon = \frac{u_{RMS}^3}{l} \tag{6}$$

where l is the eddy length scale. Because the eddy length scale in experimental ecosystems is so much smaller than in nature, energy dissipation rate quickly becomes excessively large in experimental ecosystems (Sanford 1997; Peters and Redondo 1997). Thus, energy dissipation rate ($cm^2 \, s^{-3}$) is especially difficult to keep at low enough levels in experimental ecosystems to be realistic.

Small-scale fluid shear is controlled by the energy dissipation rate, with consequences on processes such as planktonic contact rates (e.g., particulate/copepod interaction, Rothschild and Osborn 1988; MacKenzie et al. 1994; Kiørboe 1997) and the aggregation and disaggregation of particles (Hill et al. 1992; Riebesell and Wolf Gadrow 1992). Without realistic energy dissipation rates, distortion of ecosystem processes by unrealistic rates of interactions can yield results of limited value. As outlined by Peters and Redondo (1997) many mesocosm studies with mixing were strongly overmixed with unrealistically high energy dissipation rates (Fig. 2).

Mesocosms with a sediment bottom to examine both WC and bottom turbulence

Recently, mesocosms to examine both WC and bottom turbulence simultaneously have been used to study benthic–pelagic coupling processes (Table 1). Dimitriou et al. (2017) designed a novel mesocosm setup for benthic–pelagic coupling experiments using an air lift system for mixing, but omitted measurement of mixing and bottom shear stress. In coupled systems, coupling a mesocosm top with an annular flume or Gust microcosm bottom, respectively, intermediate bottom shear stress (shear velocity $\sim 0.6 \, cm \, s^{-1}$) in a benthic–pelagic coupling experiment was compared to unrealistically low shear stress in tanks where all systems had similar,

realistic, WC turbulence (Porter et al. 2004*a,b*, Table 2). While the intermediate bottom shear stress was too low to result in wide-scale sediment resuspension, the intermediate bottom shear stress eroded microphytobenthos, which subsequently affected biogeochemical flux rates. Sediment resuspension studies, however, could not be performed in these coupled systems as connecting lines were not able to support a realistic and a physically reliable transport of particulates between the top and the bottom of the WC. Six scientific published studies from 2000 to 2009 used benthic–pelagic coupled systems (Fig. 5). These benthic–pelagic coupled systems used for ecological studies, had no resuspension but uniform moderate bottom shear velocity of about $0.6 \, cm \, s^{-1}$ and realistic WC mixing (Fig. 5). The benthic–pelagic coupled systems were retired after 2009.

A Benthic WC Simulator (Mueller et al. 2007) to simulate WC hydrodynamics in benthic chambers has been used for short-term aquatic resuspension-deposition cycling studies (Kleeberg et al. 2013; Kleeberg and Herzog 2014); however, the device is small and not suited for long-term experiments.

Conventional approaches to understanding the coupling of benthic and pelagic processes are limited by the complexity of indirect and non-linear processes that control interactions (Wootton 2002; Krivtsov 2004; Porter et al. 2004*a*; Najjar et al. 2010). Interactions between different components of the aquatic community can be complex and properly designed experiments may reveal ecological behavior beyond the capability of current mathematical modeling (Cadotte et al. 2005). Shear turbulence resuspension mesocosms (STURM, Porter
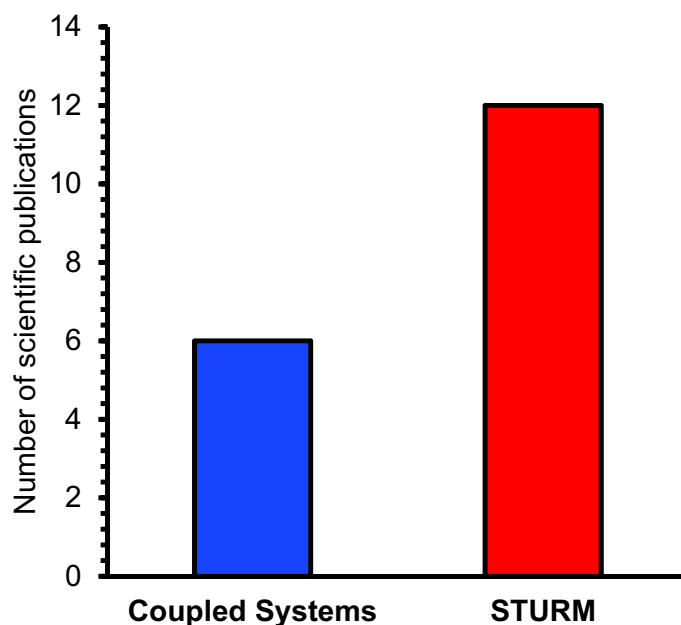
Fig. 5. Number of scientific published studies from 2000 to 2009 using coupled systems and from 2004 to 2022 using STURM for ecological studies. Note scale.

et al. 2018*a*,*b*, Fig. 6) were designed to incorporate indirect interactions in ecosystem experiments. In STURM systems, bottom shear stress is high and WC turbulence levels are kept at realistic levels. In particular, energy dissipation rates are difficult to keep at low enough levels in experimental ecosystems to be realistic, as they scale nonlinearly with RMS turbulent velocity (see section 6, Table 4, Eq. 6). The ratio of RMS turbulent velocity to the instantaneous spikes of shear velocity ranges from 0.25 to 1.05 in the STURM tanks (Table 2). This is close to the ratio of RMS turbulent velocity and bottom shear velocity ratio of $\sim 1.4 : 1$ in nature (Table 2), and much improved over the ratio of $7-7.5 : 1$ in traditional isolated tank mesocosms (Table 2) where the bottom and the WC are poorly connected. Twelve ecological scientific benthic–pelagic coupling studies published from 2004 to 2022 have used STURM with high bottom shear stress and realistic RMS turbulent velocity and energy dissipation rates (Fig. 6).

For benthic–pelagic coupling, the cycling of particulate organic matter between the sediments and the WC and any direct and indirect feedback effects on the ecosystem are important for food webs and carbon and nitrogen cycling (Porter et al. 2018*b*, 2020*a*, 2022). In STURM tanks with high

bottom shear stress and resuspension of organic-rich oyster biodeposits and sediments, biogeochemical processes dominated in the WC and affected the oxygen and the nitrogen dynamics in the ecosystem (Porter et al. 2022). In contrast, sediment biogeochemical processes dominated in the non-resuspension systems, identical in WC turbulence (RMS turbulent velocity and energy dissipation rate) to the STURM systems, but that had low bottom shear stress (Porter et al. 2022). Oyster biodeposit resuspension in a different STURM experiment affected the seston, nutrient, phytoplankton, and zooplankton dynamics (Porter et al. 2018*b*).

Moreover, oyster biodeposit resuspension affected phytoplankton community structure in another STURM experiment (Porter et al. 2020*a*) and the benthic–pelagic connection proved important for phytoplankton. In an experiment focusing on the phytoplankton and zooplankton dynamics in response to sediment and biodeposit resuspension, muddy sediment and high bottom shear stress with resuspension were run in six STURM tanks over a four-week period, where three of the tanks included a daily oyster biodeposit addition and resuspension (Porter et al. 2020*a*). In STURM tanks without biodeposit resuspension (Porter et al. 2020*a*),

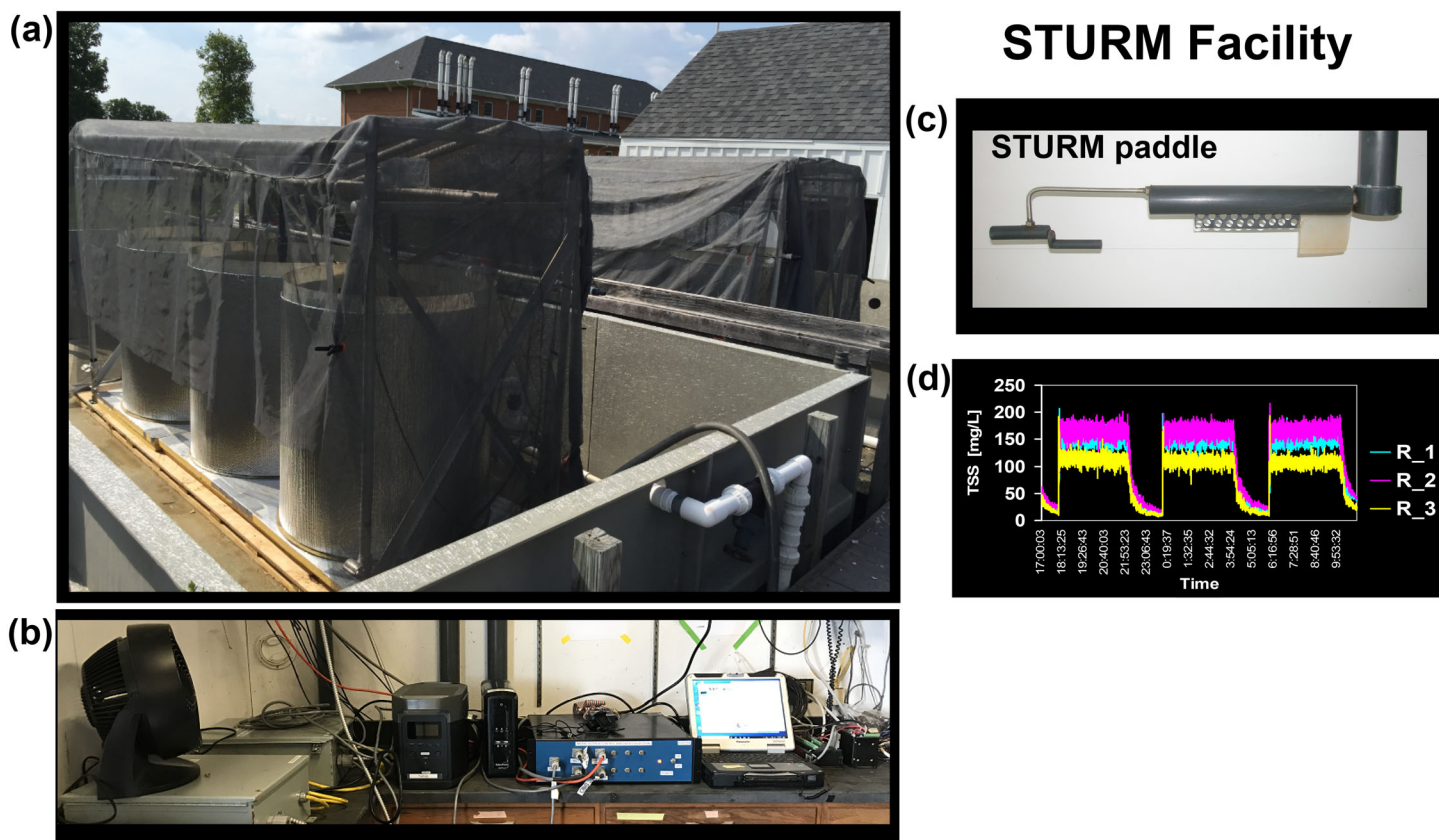**Fig. 6.** (**a**) Current setup of the STURM facility at the Patuxent Environmental and Aquatic Research Laboratory with shading for a summer experiment, (**b**) mixing and data control center, (**c**) STURM paddle to create WC turbulence and bottom shear stress, and (**d**) example of mimicked tidal resuspension, total suspended solids concentrations in resuspension (R) tanks (after Porter et al. 2018*a*).

phytoplankton biomass, dominated by a bloom of *Skeletonema costatum* with long chains, was enhanced compared to STURM tanks with biodeposit resuspension. In addition, zooplankton biomass was lower, suggesting that zooplankton were not able to feed on *S. costatum* and/or were negatively affected by *S. costatum*.

In contrast, in STURM tanks with biodeposit resuspension (Porter et al. 2020*a*), zooplankton biomass (dominated by *Acartia tonsa*) was enhanced and *S. costatum* abundance reduced compared to tanks without biodeposit resuspension. Moreover, *S. costatum* had shorter chains. In these tanks with biodeposit resuspension, phytoplankton carbon was efficiently transferred to zooplankton. In tanks with biodeposit resuspension, the pelagic food web was enhanced. This experiment illustrated the importance of conducting mesocosm experiments with high bottom shear stress and a benthic–pelagic connection dissimilar to previous studies reviewed by Arnott et al. (2021).

Sediment erodibility as affected by infaunal bivalve density of the hard clam *Mercenaria mercenaria*, was measured in microcosm erosion devices and STURM tanks (Porter et al. 2020*b*) and found that a high density of infaunal bivalves increased sediment erodibility. In the whole ecosystem context, a high density of infaunal bivalves led to high sediment resuspension, affecting water clarity and microphytobenthos biomass as well as the nitrogen dynamics in a 4-week ecosystem experiment and thus included important direct and indirect feedbacks (Porter et al. 2013).

Benthic–pelagic coupling experiments in three STURM tanks with polychlorinated biphenyls (PCB) in the sediment where the time between storm events was varied found that with infrequent resuspension events, the labile PCB pool gets replenished and PCB released into the WC (Schneider et al. 2007). Thus, PCB release could be affected by storm frequency. Mercury bioaccumulation in hard clams, *Mercenaria mercenaria*, and zooplankton in a resuspension experiment in STURM tanks indicated that sediment resuspension can play an important role in transferring sediment methyl mercury into organisms through direct and indirect interactions (Kim et al. 2006). In an additional STURM experiment to determine the effect of resuspension on the cycling of total mercury and methyl mercury between the WC and the sediment, an experiment comparing resuspension systems vs. non-resuspension systems was conducted where the tanks differed in bottom shear stress but all had similar, realistic WC turbulence (RMS turbulent velocity and energy dissipation rate; Kim et al. 2004). The results suggested that total mercury was mostly bound to sediment particles with very little release during the resuspension events (Kim et al. 2004).

By manipulating wave amplitude and wavelength in a flow channel, Hulot et al. (2017) proposed making realistic wave climates in low-cost mesocosms as a new tool for experimental ecology and biogeomorphology. While Hulot et al. (2017) suggest high bottom shear stress can be produced in the wave

mesocosms (or "wave flumes"); RMS turbulent velocity and energy dissipation rate were not measured. When wave amplitude increased, the standard deviation of water velocity similarly increased for a given wavelength (Hulot et al. 2017). The standard deviation decreased with water depth, although this decrease was less pronounced for large wavelengths (2.5 and 5 m, Hulot et al. 2017).

In outdoor rectangular ($10 \times 1.5 \times 1.5$ m) wave mesocosms, Blottière et al. (2017) simulated a resuspension treatment where they generated long wavelength waves (c. 3.5 m) to mix the entire WC and create high bottom shear stress so that the surface layers of sediment would be resuspended; however bottom shear stress was unmeasured. In addition, in three additional wave mesocosms Blottière et al. (2017) mimicked a non resuspension treatment with short wavelength waves. They successfully produced resuspension and found significantly higher chlorophyll *a* concentrations in the resuspension treatment than in the non resuspension treatment, similar to the resuspension treatment in STURM systems (Porter et al. 2010). In outdoor rectangular ($10 \times 1.5 \times 1.5$ m) wave mesocosms, Blottière et al. (2017) simulated a resuspension treatment where they generated long wavelength waves (c. 3.5 m) to mix the entire WC and create high bottom shear stress so that the surface layers of sediment would be resuspended; however, bottom shear stress was unmeasured. While these wave mesocosms presumably mimic a whole WC and are able to generate waves from 0.1 to 6 m of wavelength and 1–5 cm of amplitude with a 1 m WC, bottom shear stress, RMS turbulent velocity, and energy dissipation rate were not quantified.

Marin-Diaz et al. (2019) used a 3.5 m long, 0.6 m wide, and 0.8 m deep hydraulic wave flume developed and constructed at the Netherlands Institute for Sea Research (NIOZ) and located at Kristineberg Marine Research Station for a study on the role of eelgrass on bed-load transport and sediment resuspension under oscillatory flow. Turbidity and a decrease of light in the WC were measured to determine the critical erosion threshold (Marin-Diaz et al. 2019); however, shear stress was not quantified. Marin-Diaz (2019) measured mean orbital velocities U_{RMS} in the WC, which ranged up to 28 cm s^{-1} over bare mud and bare sand but energy dissipation rate was not measured.

Infantes et al. (2021) followed up on the design used by Marin-Diaz et al. (2019), compared the wave mesocosm to a natural wave environment, and found that a range of realistic relevant regular and irregular wave conditions could be generated. Infantes et al. (2021) were able to mimic constant realistic wave-induced bottom shear stress such as found in the field. Moreover, bottom shear stress and orbital velocity (Table 5) combinations in their inexpensive wave mesocosm were close to those found in nature (Infantes et al. 2021). Their wave mesocosm was found to realistically mimic maximum orbital velocities of 10–50 cm s^{-1} and short wave conditions ($T_p = 1$–3 s) as found in estuaries, lakes, or fjords (Infantes

et al. 2021). They measured also RMS turbulent velocity but did not assess energy dissipation rate. Total kinetic energy (TKE) ranged from 0.8 to 30 $cm^2 s^{-2}$ where their $TKE = \frac{3}{2} u_{RMS}^2$ (Infantes et al. 2021). Mimicking hydrodynamically accurate wave conditions is less important than constant wave-induced shear stress for realistically representing ecological and biogeomorphological processes (Infantes et al. 2021). To summarize, wave mesocosms can be used for ecological short-term and longer-term (weeks to months) benthic–pelagic coupling experiments with realistic shear stress-orbital velocity combinations, however, energy dissipation should also be measured.

Overall, the number of engineering wave flume investigations has increased dramatically from 1985 to 2019, followed by a slow start of wave flume experiments in ecological disciplines (Infantes et al. 2021, Fig. 7). Overall, there is a great lack of ecological benthic–pelagic coupling studies in mesocosms that include turbulence and scale both, mixing in the WC and at the benthos.

Future applications

The exchange of nutrients and oxygen between the benthic ecosystem and the WC ecosystem can provide 1) a large "internal" source of nutrients to support WC productivity (Porter et al. 2010; Moriarty et al. 2017, 2018) and 2) a sink for oxygen (Porter et al. 2022; Moriarty et al. 2017, 2018), with the associated issues with biogeochemical (Breitburg et al. 2018) and biological effects (Breitburg et al. 2003, 2009) of low oxygen. We describe here several areas where coupled WC and sediment studies may benefit from a more realistic experimental physical regime.

Boundary-layer flow without resuspension

The penetration of oxygen into sediments is critical to biogeochemical processes such as coupled nitrification–denitrification (Rysgaard et al. 1994), re-oxidation of ferrous iron and other reduced species (i.e., dissolved H_2S and iron sulfide minerals (Glud 2008), and adsorption of soluble reactive phosphorus (Karstens et al. 2015). Most studies of boundary layer physics have emphasized resuspension, but compression of the benthic boundary layer can decrease the diffusive distance to total oxygen depletion. In sediments with low rates of oxygen uptake, changes in the benthic boundary layer thickness have a minimal proportional effect on the total diffusive path length (Cai and Sayles 1996) and would have little impact on benthic fluxes of solutes and gases. In sediments with high oxygen demand, the short diffusive pathway of oxygen within the sediments would be strongly affected by the diffusion distance of oxygen within the benthic boundary layer. Systems with high sediment oxygen demand occur where high rates of algal deposition occur (Davis et al. 1987); but the effect of turbulent flow on sediment fluxes and WC productivity have not been addressed.
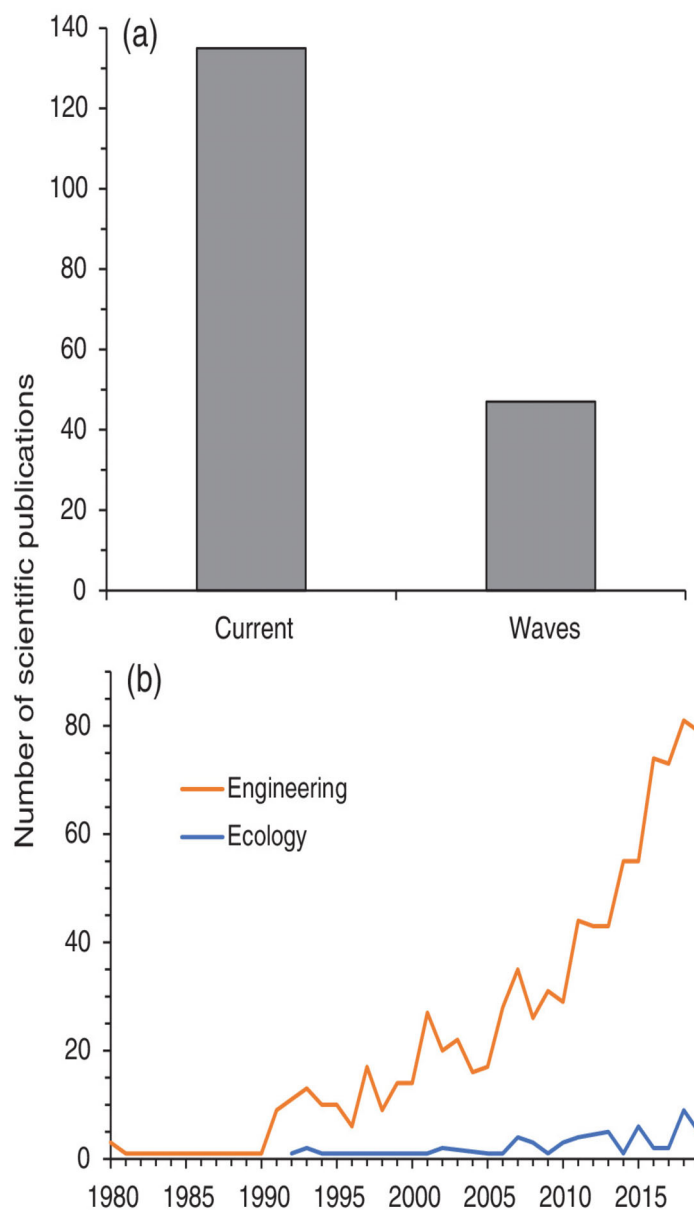

Fig. 7. Number of scientific published studies from 1985 to 2019 on (**a**) ecological studies using current and wave flumes. (**b**) Yearly publications in engineering and ecological disciplines using wave flumes (Web of Science). From Infantes et al. 2021. http://creativecommons.org/licenses/by/4.0/.

Boundary-layer flow with resuspension

The resuspension of sediments from the most reactive layer can impact the net balance of oxygen, dissolved inorganic carbon and nutrients (Almroth et al. 2009; Almroth-Rosell et al. 2012; Porter et al. 2022). Many resuspension experiments use uncalibrated physics, with resuspension derived from increased rotation of the stirring system (Almroth et al. 2009; Wang et al. 2018) or shaking (Ståhlberg et al. 2006; Da-Peng and Yong 2010; Acquavita et al. 2012). The short-term impacts

of resuspension can include elevated rates of oxygen uptake and nutrient release (Almroth et al. 2009; Porter et al. 2010, 2022). Some aspects of sediment resuspension on biogeochemical processes would benefit from studies in a coupled WC/sediment system. Resuspension of chemical species in the very top layer of sediment can result in an instantaneous elevated release of nutrient elements (Couceiro et al. 2013) and/or enhanced oxidation of reduced species such as dissolved or solid phase Fe(II) or S(II) within the WC (Simpson et al. 1998). The introduction of oxygen into deeper sediment horizons that were uncovered by resuspension can also result in increased oxygen uptake at the sediment–water interface. However, the effects of a resuspension "event" on longer term nutrient and oxygen balances may be counter balanced by decreased fluxes immediately afterward. Porewater gradients would need to be rebuilt after the event and for soluble reactive P, increased adsorption to Fe oxides may occur at a more oxidized sediment surface. In a study by Schneider et al. (2007) in STURM systems, after the first resuspension event, the solids were allowed to settle and the quiescent time was varied to determine whether the labile pool of PCBs is recharged during sediment consolidation. It was found that the easily desorbable PCBs recharge when there is sufficient time between resuspension events (Schneider et al. 2007); however, nutrients were not measured. Short-term changes in oxygen profiles (Jørgensen et al. 2022), and resuspension of the nitrifying microbial community (Xia et al. 2017*a*), can result in changes in rates of nitrification and denitrification (Xia et al. 2017*b*). Depuration of adsorbed ammonium from suspended particles, as well as the new sediment surface, may alter the nitrogen cycle.

Benthic–pelagic coupling relevant to harmful algae studies

Cyanobacterial blooms present challenges to both ecological (Rastogi et al. 2015) and human health (Metcalf et al. 2018), with a need to understand their causes and the efficacy of mitigation approaches. The WC physical regime is critical to cyanobacteria, with processes of vertical mixing/buoyancy (Walsby et al. 1997; Bormans et al. 1999) and washout (Mitrovic et al. 2010) being important controls of bloom persistence. Sediments can also be important to bloom formation and persistence, with elevated pH with blooms resulting in altered P and N resupply from the sediments (Seitzinger 1991; Gao et al. 2012, 2014), and as a site for resting stages (Yamamoto 2010; Ellegaard and Riberio 2018). With the potential "seed" bank in sediments critical to bloom initiation, potentially enhanced by resuspension, experiments with sediments collected beneath blooms may provide clues on conditions that promote cyanobacterial bloom formation. Efforts to curb blooms include addition of WC inhibitors and algaecides (Zhou et al. 2018; Sukenik and Kaplan 2021; Zhu et al. 2021), aeration and mixing (Piehler 2008; Schõnach et al. 2017) and phosphorus adsorbents (Li et al. 2021). A combined WC and sediment system with realistic and experimentally controllable physics

may provide an optimal experimental system for studying shallow water blooms and their mitigation.

Biogeochemical studies of reservoir infill and effects of dredging

The interception of sediments and nutrients by reservoirs is often a function of the physical regime (Chung et al. 2008; Palinkas and Russ 2019) and the water residence time (Vörösmarty et al. 2003; Cook et al. 2009; Bouwman et al. 2013). In the lower Susquehanna River drainage, reservoirs more efficiently trapped sediment in the past, with infill shallowing the reservoir and decreasing ongoing sediment retention (Zhang et al. 2013; Palinkas et al. 2019) and possibly leading to a lower scour threshold during high flow events. Initial deposition, followed by wind-driven resupension and downstream transport can redistribute the most reactive particulate material within the sediments and alter sediment metabolic rates. Potential mitigation via dredging needs to account for surficial sediment dynamics. Coupled sediment-WC experiment systems may be useful to calibrate the models. Although small-scale experimental systems cannot replicate the intense physical forcing of high flows from tropical storms or hurricanes, a coupled sediment-water experimental system would provide insight into how WC and sediment interfacial physics combine to either enhance nutrient retention or release.

Conclusion

Mixing in mesocosms is important and must be quantified and reported (Peters and Redondo 1997; Sanford 1997; Sanford et al. 2009). RMS turbulent velocity, energy dissipation rate and bottom shear stress should be determined. Only mesocosms that place an emphasis on both WC turbulence and bottom turbulence simultaneously should be used for benthic–pelagic coupling studies, as otherwise artifacts may arise and direct and indirect linkages may be missed. Griffiths et al. (2017) point out the importance of benthic–pelagic coupling for marine ecosystem functioning in a changing world. Griffiths et al. (2017) suggest that human-induced nutrient loading, climate change and fishing must be investigated in benthic–pelagic coupling studies, and notes that the outcomes for ecosystem function are currently poorly understood.

Models for forecasting require experimental data where the benthos and the WC are both represented realistically and benthic pelagic coupling is similar to nature (Testa et al. 2017). Models that include BPC data with feedbacks and indirect links of biogeochemical processes and food webs can give us better predictive results; however, the mechanistic understanding of benthic–pelagic processes and feedbacks is insufficient (Griffith et al. 2017; Testa et al. 2017). Mesocosm approaches where both WC turbulence and bottom turbulence are realistic can provide evidence for cause-and-effect relationships (Stewart et al. 2013).

Data availability statement

All data presented here can be found in the original sources referenced within.

References

Acquavita, A., and others. 2012. The effects of resuspension on the fate of Hg in contaminated sediments (Marano and Grado lagoon, Italy): Short-term simulation experiments. Est. Coast. Shelf Sci. **113**: 32–40.

Almroth, E., A. Tengberg, J. H. Andersson, S. Pakhomova, and P. O. J. Hall. 2009. Effects of resuspension on benthic fluxes of oxygen, nutrients, dissolved inorganic carbon, iron and manganese in the Gulf of Finland, Baltic Sea. Cont. Shelf Res. **29**: 807–818.

Almroth-Rosell, E., A. Tengberg, S. Andersson, A. Apler, and P. O. J. Hall. 2012. Effects of simulated natural and massive resuspension on benthic oxygen, nutrient and dissolved inorganic carbon fluxes in loch Creran, Scotland. J. Sea Res. **72**: 38–48.

Andersen, T. J. 2001. Seasonal variation in erodibility of two temperate, microtidal mudflats. Est. Coast. Shelf Sci. **53**: 1–12.

Arnott, R. N., M. Cherif, L. D. Bryant, and D. J. Wain. 2021. Artificially generated turbulence: A review of phycological nanocosm, microcosm, and mesocosm experiments. Hydrobiologia **848**: 961–991.

Baumert, H., and G. Radach. 1992. Hysteresis of turbulent kinetic energy in nonrotational tidal flows: A model study. J. Geophys. Res. **97**: 3669–3677.

Baustian, M. M., and others. 2014. Linking the bottom to the top in aquatic ecosystems: Mechanisms and stressors of benthic-pelagic coupling, p. 25–47. *In* P. F. Kemp [ed.], Eco-DAS X Symposium Proceedings, v. **3**. Association for the Sciences of Limnology and Oceanography.

Benton, T. G., M. Solan, J. M. Travis, and S. M. Sait. 2007. Microcosm experiments can inform global ecological problems. Trends Ecol. Evol. **22**: 516–521.

Berg, G., P. M. Glibert, and C.-C. Chen. 1999. Dimension effects of enclosures on ecological processes in pelagic systems. Limnol. Oceanogr. **44**: 1331–1340.

Blottière, L., M. Jaffar-Bandjee, S. Jacquet, A. Millot, and F. D. Hulot. 2017. Effects of mixing on the pelagic food web in shallow lakes. Freshw. Biol. **62**: 161–177.

Bormans, M., B. S. Sherman, and I. T. Webster. 1999. Is buoyancy regulation in cyanobacteria an adaptation to exploit separation of light and nutrients? Mar. Freshw. Res **50**: 897–906.

Bouwman, A. F., and others. 2013. Nutrient dynamics, transfer and retention along the aquatic continuum from land to ocean: Towards integration of ecological and biogeochemical models. Biogeosciences **10**: 1–22.

Bowden, K. F. 1962. Measurements of turbulence near the sea bed in a tidal current. J.Geophys. Res. **67**: 3181–3186.

Breitburg, D. L., and others. 2003. The pattern and influence of low dissolved oxygen in the Patuxent River, a seasonally hypoxic estuary. Estuaries **26**: 280–297.

Breitburg, D. L., D. W. Hondorp, L. A. Davias, and R. J. Diaz. 2009. Hypoxia, nitrogen, and fisheries: Integrating effects across local and global landscapes. Ann. Rev. Mar. Sci. **1**: 329–349.

Breitburg, D., and others. 2018. Declining oxygen in the global ocean and coastal waters. Science **359**: esam7240.

Butman, C. A., M. Frechette, W. R. Geyer, and V. R. Starczak. 1994. Flume experiments on food-supply to the blue mussel Mytilus edulis L as a function of boundary-layer flow. Limnology and Oceanography **39**: 1755–1768.

Cadotte, M. W., J. A. Drake, and T. Fukami. 2005. Constructing nature: Laboratory models as necessary tools for investigating complex ecological communities. Population dynamics and laboratory ecology. Adv. Ecol. Res **37**: 333–353.

Cai, W.-J., and F. L. Sayles. 1996. Oxygen penetration depths and fluxes in marine sediments. Mar. Chem. **52**: 123–131.

Cantwell, M. G., and R. M. Burgess. 2004. Variability of parameters measured during the resuspension of sediments with a particle entrainment simulator. Chemosphere **56**: 51–58.

Chatterjee, A., and others. 2013. Comparative dynamics of pelagic and benthic micro-algae in a coastal ecosystem. Est. Coast. Shelf Sci. **133**: 67–77.

Christie, M. C., K. R. Dyer, and P. Turner. 1999. Sediment flux and bed level measurements from a macro tidal mudflat. Est. Coast. Shelf Sci. **49**: 667–688.

Chung, S. W., I. H. Ko, and Y. K. Kim. 2008. Effect of reservoir flushing on downstream river water quality. J. Environ. Manage. **86**: 139–147.

Cook, P. L. M., K. T. Aldridge, S. Lamontagne, and J. D. Brookes. 2009. Retention of nitrogen, phosphorus and silicon in a large semi-arid riverine lake system. Biogeochemistry **99**: 49–63.

Couceiro, F., and others. 2013. Impact of resuspension of cohesive sediments at the oyster grounds (North Sea) on nutrient exchange across the sediment–water interface. Biogeochemistry **113**: 37–52.

Crawford, S. M., and L. P. Sanford. 2001. Boundary shear velocities and fluxes in the MEERC experimental ecosystems. Mar. Ecol. Prog. Ser. **210**: 1–12.

Da-Peng, L., and H. Yong. 2010. Sedimentary phosphorus fractions and bioavailability as influenced by repeated sediment resuspension. Ecol. Eng. **36**: 958–962.

Davis, W. S., L. A. Fay, and C. E. Herdendorf. 1987. Overview of USEPA/CLEAR Lake Erie sediment oxygen demand investigations during 1979. J. Great Lakes Res. **13**: 731–737.

de Smit, J. C., M. G. Kleinhans, T. Gerkema, K. R. Timmermans, and T. J. Bouma. 2020. Introducing the TiDyWAVE field flume: A method to quantify natural ecosystem resilience against future storm waves. Limnol. Oceanogr. Methods **18**: 585–598.

Dimitriou, P. D., and others. 2017. A novel mesocosm setup for benthic-pelagic coupling experiments. Limnol. Oceanogr. Methods **15**: 349–362.

Doering, P. H., C. A. Oviatt, and J. R. Kelly. 1986. The effects of the filter-feeding clam *Mercenaria mercenaria* on carbon cycling in experimental marine mesocosms. J. Mar. Res. **44**: 839–861.

Donaghay, P. L., and E. Klos. 1985. Physical, chemical and biological responses to simulated wind and tidal mixing in experimental marine ecosystems. Marine Ecology Progress Series **26**: 35–45.

Ellegaard, M., and S. Ribeiro. 2018. The long-term persistence of phytoplankton resting stages in aquatic seed banks. Biol. Rev. Camb. Philos. Soc. **93**: 166–183.

Evans, R. D. 1994. Empirical evidence of the importance of sediment resuspension in lakes. Hydrobiologia **284**: 5–12.

Gao, Y., J. C. Cornwell, D. K. Stoecker, and M. S. Owens. 2012. Effects of cyanobacterial-driven pH increases on sediment nutrient fluxes and coupled nitrification-denitrification in a shallow fresh water estuary. Biogeosciences **9**: 2697–2710.

Gao, Y., J. C. Cornwell, D. K. Stoecker, and M. S. Owens. 2014. Influence of cyanobacteria blooms on sediment biogeochemistry and nutrient fluxes. Limnol. Oceanogr. **59**: 959–971.

Glud, R. N. 2008. Oxygen dynamics of marine sediments. Mar Biol Res **4**: 243–289.

Gordon, C. M., and C. F. Dohne. 1973. Some observations of turbulent flow in a tidal estuary. J. Geophys. Res. **78**: 1971–1978.

Grant, W. D., and O. S. Madsen. 1979. Combined wave and current interaction with a rough bottom. J. Geophys. Res. Oceans Atmospheres **84**: 1797–1808.

Grant, W. D., and O. S. Madsen. 1982. Movable bed roughness in unsteady oscillatory flow. J. Geophys. Res. Oceans Atmospheres **87**: 469–481.

Grant, W. D., A. J. Williams III, and S. M. Glenn. 1984. Bottom stress estimates and their prediction on the northern California continental shelf during CODE-I: The importance of wave-current interaction. J. Phys. Oceanogr. **14**: 506–527.

Griffiths, J. R., and others. 2017. The importance of benthic-pelagic coupling for marine ecosystem functioning in a changing world. Glob. Chang. Biol. **23**: 2179–2196.

Grizzle, R. E., R. Langan, and H. Howell. 1994. Growth responses of Crassostrea virginica, Mercenaria mercenaria and Mytilus edulis to changes in water flow: A test of the "inhalant pumping speed" hypothesis. Journal of Shellfish Research **13**: 315.

Gross, T. F., and A. R. M. Nowell. 1983. Mean flow and turbulence scaling in a tidal boundary layer. Cont Shelf Res **2**: 109–126.

Gross, T. F., A. J. Williams, and E. A. Terray. 1994. Bottom boundary layer spectral dissipation estimates in the presence of wave motions. Cont. Shelf Res. **14**: 1239–1256.

Guillen, J., J. A. Jimenez, A. Palanques, V. Gracia, P. Puig, and J. A. Sanchez. 2002. Sediment resuspension across a microtidal, low-energy shelf. Cont. Shelf Res. **22**: 305–325.

Gust, G. 1988. Skin friction probes for field applications. J. Geophys. Res. Oceans **93**: 14121–14132.

Gust, G. 1990. Method of generating precisely-defined wall shearing stresses. U.S. Patent No. 4,973,165,1990.

Gust, G., and V. Mueller. 1997. Interfacial hydrodynamics and entrainment functions of currently used erosion devices, p. 149–174. *In* N. Burt, W. R. Parker, and J. Watts [eds.], Cohesive sediments. John Wiley and Sons.

He, H., Y. Kang, and Z. Liu. 2015. Nitrogen inputs enhance phytoplankton growth during sediment resuspension events: A mesocosm study. Hydrobiologia **744**: 297–305.

Hill, P. S., A. R. M. Nowell, and P. A. Jumars. 1992. Encounter rate by turbulent shear of particles similar in diameter to the Kolmogorov scale. J. Mar. Res. **50**: 643–668.

Houwing, E.-J. 2000. Morphodynamic development of intertidal mudflats: Consequences for the extension of the pioneer zone. Cont. Shelf Res. **20**: 1735–1748.

Hulot, F. D., and others. 2017. Mesocosms with wavemakers: A new device to study the effects of water mixing on lake ecology. Limnol. Oceanogr. Methods **15**: 154–165.

Infantes, E., J. C. Smit, E. Tamarit, and T. J. Bouma. 2021. Making realistic wave climates in low-cost wave mesocosms: A new tool for experimental ecology and biogeomorphology. Limnol. Oceanogr. Methods **19**: 317–330.

Joensuu, M., C. A. Pilditch, R. Harris, S. Hietanen, H. Pettersson, and A. Norkko. 2018. Sediment properties, biota, and local habitat structure explain variation in the erodibility of coastal sediments. Limnol. Oceanogr. **63**: 173–186.

Johnson, G. C., R. G. Lueck, and T. B. Sanford. 1994. Stress on the Mediterranean outflow plume: Part 2. Turbulent dissipation and shear measurements. J. Phys. Oceanogr. **24**: 2084–2092.

Jones, I., I. Growns, A. Arnold, S. McCall, and M. Bowes. 2015. The effects of increased flow and fine sediment on hyporheic invertebrates and nutrients in stream mesocosms. Freshw. Biol. **60**: 813–826.

Jørgensen, B. B., F. Wenzhöfer, M. Egger, and R. N. Glud. 2022. Sediment oxygen consumption: Role in the global marine carbon cycle. Earth Sci. Rev: **228**: 103987.

Kalnejais, L. H., W. R. Martin, P. Signell, and M. H. Bothner. 2007. Role of sediment resuspension in the remobilization of particulate-phase metals from coastal sediments. Environ. Sci. Technol. **41**: 2282–2288.

Kang, Y., X. Song, and Z. Liu. 2013. Sediment resuspension dampens the effect of nutrient inputs on the phytoplankton community: A mesocosm experiment study. Hydrobiologia **710**: 117–127.

Karle, I.-M., and others. 2007. Verification of a benthic boxcosm system with potential for extrapolating experimental results to the field. J. Exp. Mar. Biol. Ecol. **353**: 265–278.

Karstens, S., U. Buczko, and S. Glatzel. 2015. Phosphorus storage and mobilization in coastal Phragmites wetlands: Influence of local-scale hydrodynamics. Est. Coast. Shelf Sci. **164**: 124–133.

Kim, E. H., R. P. Mason, E. T. Porter, and H. L. Soulen. 2004. The effect of resuspension on the fate of total mercury and methyl mercury in a shallow estuarine ecosystem: A mesocosm study. Mar. Chem. **86**: 121–137.

Kim, E.-H., R. P. Mason, E. T. Porter, and H. L. Soulen. 2006. The impact of resuspension on sediment mercury dynamics, and methylmercury production and fate: A mesocosm study. Mar. Chem. **102**: 300–315.

Kiørboe, T. 1997. Small-scale turbulence, marine snow formation, and planktivorous feeding. Sci Marine. **61-Supl 1**: 141–158.

Kleeberg, A., M. Hupfer, G. Gust, I. Salka, K. Pohlmann, and H.-P. Grossart. 2013. Intermittent riverine resuspension: Effects on phosphorus transformations and heterotrophic bacteria. Limnol. Oceanogr. **58**: 635–652.

Kleeberg, A., and C. Herzog. 2014. Sediment microstructure and resuspension behavior depend on each other. Biogeochemistry **119**: 199–213.

Krivtsov, V. 2004. Investigations of indirect relationships in ecology and environmental sciences: A review and the implications for comparative theoretical ecosystem analysis. Ecol. Model. **174**: 37–54.

Latimer, J. S., W. R. Davis, and D. J. Keith. 1999. Mobilization of PAHS and PCBs from in-place contaminated marine sediments during simulated resuspension events. Est. Coast. Shelf Sci. **49**: 577–595.

Law, B. A., P. S. Hill, T. G. Milligan, and V. Zions. 2016. Erodibility of aquaculture waste from different bottom substrates. Aquacult. Env. Interac. **8**: 575–584.

Li, J., K. Sellner, A. Place, J. Cornwell, and Y. Gao. 2021. Mitigation of CyanoHABs using Phoslock® to reduce water column phosphorus and nutrient release from sediment. Int. J. Environ. Res. Public Health **18**: 13360.

Maa, J. P.-Y., L. D. Wright, C.-H. Lee, and T. W. Shannon. 1993. VIMS Sea carousel: A field instrument for studying sediment transport. Mar. Geol. **115**: 271–287.

Maa, J. P.-Y., L. P. Sanford, and J. P. Halka. 1998. Sediment resuspension characteristics in Baltimore Harbor, Maryland. Mar. Geol. **146**: 137–145.

MacKenzie, B. R., and W. C. Leggett. 1993. Wind-based models for estimating the dissipation rates of turbulent energy in aquatic environments: Empirical comparisons. Mar. Ecol. Prog. Ser. **94**: 207–216.

MacKenzie, B. R., T. J. Miller, S. Cyr, and W. C. Leggett. 1994. Evidence for a dome-shaped relationship between turbulence and larval fish ingestion rates. Limnol. Oceanogr. **39**: 1790–1799.

Marin-Diaz, B., T. J. Bouma, and E. Infantes. 2019. Role of eelgrass on bed-load transport and sediment resuspension under oscillatory flow. Limnol. Oceanogr. **65**: 426–436.

Metcalf, J. S., and others. 2018. Public health responses to toxic cyanobacterial blooms: Perspectives from the 2016 Florida event. Water Policy **20**: 919–932.

Meysick, L., E. Infantes, L. Rugiu, K. Gagnon, and C. Boström. 2022. Coastal ecosystem engineers and their impact on sediment dynamics: Eelgrass–bivalve interactions under wave exposure. Limnol. Oceanogr. **67**: 621–633.

Mitrovic, S. M., L. Hardwick, and F. Dorani. 2010. Use of flow management to mitigate cyanobacterial blooms in the lower Darling River, Australia. J. Plankton Res. **33**: 229–241.

Moriarty, J. M., C. K. Harris, K. Fennel, M. A. M. Friedrichs, K. Xu, and C. Rabouille. 2017. The roles of resuspension, diffusion and biogeochemical processes on oxygen dynamics offshore of the Rhône River, France: A numerical modeling study. Biogeosciences **14**: 1919–1946.

Moriarty, J. M., C. K. Harris, M. A. M. Friedrichs, K. Fennel, and K. Xu. 2018. Impact of seabed resuspension on oxygen and nitrogen dynamics in the northern Gulf of Mexico: A numerical modeling study. J. Geophys. Res. Oceans **123**: 7237–7263.

Moriarty, J. M., M. A. M. Friedrichs, and C. K. Harris. 2020. Seabed resuspension in the Chesapeake Bay: Implications for biogeochemical cycling and hypoxia. Estuaries Coasts **44**: 103–122.

Mueller, V., A. Seibel, D. Kisacik, and G. Gust. 2007. Simulation of water column hydrodynamics by benthic chambers, p. 90–99. *In* U. Foerstner and B. Westrick [eds.], Sediment dynamics and pollutant mobility in rivers–an interdisciplinary approach. Springer-Verlag.

Muschenheim, D. K., J. Grant, and E. L. Mills. 1986. Flumes for benthic ecologists: theory, construction and practice. Marine Ecology Progress Series **28**: 185–196.

Najjar, R. G., and others. 2010. Potential climate-change impacts on the Chesapeake Bay. Est. Coast. Shelf Sci. **86**: 1–20.

Nixon, S. W., D. Alonso, M. E. Q. Pilson, and B. A. Buckley. 1980. Turbulent Mixing in Aquatic Microcosms, p. 818–849. *In* J. P. Giesy [ed.], Microcosms in ecological research. DOE Symposium Series. Technical Information Center, U.S. Department of Energy.

Nowell, A. R. M., and P. A. Jumars. 1987. Flumes: Theoretical and experimental considerations for simulation of benthic environments. Oceanography and Marine Biology Annual Review **25**: 91–112.

Orlins, J. J., and J. S. Gulliver. 2003. Turbulence quantification and sediment resuspension in an oscillating grid chamber. Exp. Fluids **34**: 662–677.

Oviatt, C. A., C. D. Hunt, G. A. Vargo, and K. W. Kopchynski. 1981. Simulation of a storm event in marine microcosms. J. Mar. Res. **39**: 605–626.

Palinkas, C. M., and E. Russ. 2019. Spatial and temporal patterns of sedimentation in an infilling reservoir. Catena **180**: 120–131.

Palinkas, C. M., J. M. Testa, J. C. Cornwell, M. Li, and L. P. Sanford. 2019. Influences of a river dam on delivery and fate of sediments and particulate nutrients to the adjacent estuary: Case study of Conowingo dam and Chesapeake Bay. Estuaries Coasts **42**: 2072–2095.

Peters, F., and J. M. Redondo. 1997. Turbulence generation and measurement: Application to studies on plankton. Sci. Mar. **61**: 205–228.

Petersen, J. E., J. C. Cornwell, and W. M. Kemp. 1999. Implicit scaling in the design of experimental aquatic ecosystems. Oikos **85**: 3–18.

Petersen, J. E., and others. 2003. Multiscale experiments in coastal ecology: Improving realism and advancing theory. Bioscience **53**: 1181.

Piehler, M. F. 2008. Watershed management strategies to prevent and control cyanobacterial harmful algal blooms, p. 259–273. *In* H. K. Hudnell [ed.], Cyanobacterial harmful algal blooms: State of the science and research needs. Springer.

Pollingher, U., and E. Zemel. 1981. In situ and experimental evidence of the influence of turbulence on cell division processes *of Peridinium cinctum forma westii* (Lemm.) Lefèvre. Br. Phycol. J. **16**: 281–287.

Porter, E. T., L. P. Sanford, G. Gust, and F. S. Porter. 2004*a*. Combined water-column mixing and benthic boundary-layer flow in mesocosms: Key for realistic benthic-pelagic coupling studies. Mar. Ecol. Prog. Ser. **271**: 43–60.

Porter, E. T., J. C. Cornwell, L. P. Sanford, and R. I. E. Newell. 2004*b*. Effect of oysters *Crassostrea virginica* and bottom shear velocity on benthic-pelagic coupling and estuarine water quality. Mar. Ecol. Prog. Ser. **271**: 61–75.

Porter, E. T., L. P. Sanford, F. S. Porter, and R. P. Mason. 2018*a*. STURM: Resuspension mesocosms with realistic bottom shear stress and water column turbulence for benthic-pelagic coupling studies: Design and applications. J. Exp. Mar. Biol. Ecol. **499**: 35–50.

Porter, E. T., H. Franz, and R. Lacouture. 2018*b*. Impact of eastern oyster *Crassostrea virginica* biodeposit resuspension on the seston, nutrient, phytoplankton, and zooplankton dynamics: A mesocosm experiment. Mar. Ecol. Prog. Ser. **586**: 21–40.

Porter, E. T., E. Robins, S. Davis, R. Lacouture, and J. C. Cornwell. 2020*a*. Effects of resuspension of eastern oyster *Crassostrea virginica* biodeposits on phytoplankton community structure. Mar. Ecol. Prog. Ser. **640**: 79–105.

Porter, E. T., B. J. Johnson, and L. P. Sanford. 2020*b*. Effects of hard clam (*Mercenaria mercenaria*) density and bottom shear stress on cohesive sediment erodibility and implications for benthic-pelagic coupling. J. Mar. Res. **78**: 91–130.

Porter, E. T., R. P. Mason, and L. P. Sanford. 2010. Effect of tidal resuspension on benthic-pelagic coupling in an experimental ecosystem study. Mar. Ecol. Prog. Ser. **413**: 33–53.

Porter, E. T., R. P. Mason, and L. P. Sanford. 2013. Effects of shear stress and hard clams on seston, microphytobenthos, and nitrogen dynamics in mesocosms with tidal resuspension. Mar. Ecol. Prog. Ser. **479**: 25–46.

Porter, E. T., S. Blickenstaff, J. C. Cornwell, M. Jackson, and S. N. Tolbert. 2022. Effect of tidal resuspension with oyster biodeposits on nutrient and oxygen dynamics. Mar. Ecol. Prog. Ser. **686**: 37–60.

Rastogi, R. P., D. Madamwar, and A. Incharoensakdi. 2015. Bloom dynamics of cyanobacteria and their toxins: Environmental health impacts and mitigation strategies. Front. Microbiol. **6**: 1254.

Riebesell, U., and D. A. Wolf-Gladrow. 1992. The relationship between physical aggregation of phytoplankton and particle flux: A numerical model. Deep Sea Res. **39**: 1085–1102.

Rothschild, B. J., and T. R. Osborn. 1988. Small-scale turbulence and plankton contact rates. J. Plankton Res. **10**: 465–474.

Rysgaard, S., N. Risgaard-Petersen, S. Niels Peter, J. Kim, and N. Lars Peter. 1994. Oxygen regulation of nitrification and denitrification in sediments. Limnol. Oceanogr. **39**: 1643–1652.

Sanford, L. P. 1997. Turbulent mixing in experimental ecosystems. Mar. Ecol. Prog. Ser. **161**: 265–293.

Sanford, L. P., W. Panageotou, and J. P. Halka. 1991. Tidal resuspension of sediments in northern Chesapeake Bay. Mar. Geol. **97**: 87–103.

Sanford, L. P., and J. P. Halka. 1993. Assessing the paradigm of mutually exclusive erosion and deposition of mud, with examples from upper Chesapeake Bay. Mar. Geol. **114**: 37–57.

Sanford, L. P., S. E. Suttles, and E. T. Porter. 2009. Physical factors: Mixing and flow, p. 63–74. *In* J. E. Petersen, V. S. Kennedy, W. C. Dennison, and W. M. Kemp [eds.], Enclosed experimental ecosystems and scale. Tools for understanding and managing coastal ecosystems. Springer.

Santschi, P. H. 1985. The merl mesocosm approach for studying sediment-water interactions and ecotoxicology. Environ. Technol. Lett. **6**: 335–350.

Savidge, G. 1981. Studies of the effects of small-scale turbulence on phytoplankton. J. Mar. Biol. Ass. **61**: 477–488.

Schindler, D. E., and M. D. Scheuerell. 2002. Habitat coupling in Lake ecosystems. Oikos **98**: 177–189.

Schneider, A. R., E. T. Porter, and J. E. Baker. 2007. Polychlorinated biphenyl release from resuspended Hudson River sediment. Environ. Sci. Technol. **41**: 1097–1103.

Schönach, P., and others. 2017. Persistency of artificial aeration at hypertrophic Lake Tuusulanjarvi: A sociohistorical analysis. Ambio **46**: 865–877.

Seitzinger, S. P. 1991. The effect of pH on the release of phosphorus from Potomac estuary sediments: Implications for blue-green algal blooms. Est. Coast. Shelf Sci. **33**: 409–418.

Sharma, K. V., B. K. Sarvalingam, and S. R. Marigoudar. 2021. A review of mesocosm experiments on heavy metals in marine

environment and related issues of emerging concerns. Environ. Sci. Pollut. Res. Int. **28**: 1304–1316.

Simpson, S. L., S. C. Apte, and G. E. Batley. 1998. Effect of short-term resuspension events on trace metal speciation in polluted anoxic sediments. Environ. Sci. Technol.: **32**: 620–625.

Sloth, N. P., B. Riemann, L. P. Nielsen, and T. H. Blackburn. 1996. Resilience of pelagic and benthic microbial communities to sediment resuspension in a coastal ecosystem, Knebel Vig, Denmark. Est. Coast. Shelf Sci. **42**: 405–415.

Spivak, A. C., M. J. Vanni, and E. M. Mette. 2011. Moving on up: Can results from simple aquatic mesocosm experiments be applied across broad spatial scales? Freshw. Biol. **56**: 279–291.

Ståhlberg, C., D. Bastviken, B. H. Svensson, and L. Rahm. 2006. Mineralisation of organic matter in coastal sediments at different frequency and duration of resuspension. Est. Coast. Shelf Sci. **70**: 317–325.

Stewart, R. I. A., and others. 2013. Mesocosm experiments as a tool for ecological climate-change research. Adv Ecol Res **48**: 71–181.

Striebel, M., L. Kirchmaier, and P. Hingsamer. 2013. Different mixing techniques in experimental mesocosms-does mixing affect plankton biomass and community composition? Limnol. Oceanogr. Methods **11**: 176–186.

Sukenik, A., and A. Kaplan. 2021. Cyanobacterial harmful algal blooms in aquatic ecosystems: A comprehensive outlook on current and emerging mitigation and control approaches. Microorganisms **9**: 1472.

Sutherland, A. B. 2006. A simple reciprocating apparatus for maintaining long-term turbidity in biological experiments. Limnol. Oceanogr. Methods **4**: 49–57.

Tengberg, A., and others. 2004. Intercalibration of benthic flux chambers I. accuracy of flux measurements and influence of chamber hydrodynamics. Prog. Oceanogr. **60**: 1–28.

Tennekes, H., and J. L. Lumley. 1972. A first course in turbulence. MIT Press.

Terray, E. A., and others. 1996. Estimates of kinetic energy dissipation under breaking waves. J. Phys. Oceanogr. **26**: 792–807.

Testa, J. M., W. M. Kemp, L. A. Harris, R. J. Woodland, and W. R. Boynton. 2017. Challenges and directions for the advancement of estuarine ecosystem science. Ecosystems **20**: 14–22.

Threlkeld, S. T. 1994. Benthic-pelagic interactions in shallow water columns: An experimentalist's perspective. Hydrobiologia **275**: 293–300.

Tsai, C.-H., and W. Lick. 1986. A portable device for measuring sediment resuspension. J. Great Lakes Res. **12**: 314–321.

Vadeboncoeur, Y., M. J. Vander Zanden, and D. M. Lodge. 2002. Putting the lake back together: Reintegrating benthic pathways into lake food web models. Bioscience **52**: 44–54.

von Bodungen, B., K. von Broeckel, V. Smetacek, and B. Zeitschel. 1976. The plankton tower. I. a structure to study water/sediment interactions in enclosed water columns. Mar. Biol. **34**: 369–372.

Vörösmarty, C. J., M. Meybeck, B. Fekete, K. Sharma, P. Green, and J. P. M. Syvitski. 2003. Anthropogenic sediment retention: Major global impact from registered river impoundments. Global Planet. Change **39**: 169–190.

Walsby, A. E., P. K. Hayes, R. Boje, and L. J. Stal. 1997. The selective advantage of buoyancy provided by gas vesicles for planktonic cyanobacteria in the Baltic Sea. New Phytol. **136**: 407–417.

Wang, J., J. Xu, J. Xia, F. Wu, and Y. Zhang. 2018. A kinetic study of concurrent arsenic adsorption and phosphorus release during sediment resuspension. Chem. Geol. **495**: 67–75.

Wengrove, M. E., D. L. Foster, L. Kalnejais, Percuoco, and T. C. Lippmann. 2015. Field and laboratory observations of bed stress and associated nutrient release in a tidal estuary. Est. Coast.Shelf Sci. **161**: 11–24.

White, A. W. 1976. Growth inhibition caused by turbulence in the toxic marine dinoflagellate Gonyaulax excavata. J. Fish. Res. Board Can. **33**: 2598–2602.

Widdows, J., M. D. Brinsley, P. N. Salkeld, and M. Elliott. 1998. Use of annular flumes to determine the influence of current velocity and bivalves on material flux at the sediment-water interface. Estuaries **21**: 552–559.

Widdows, J., M. D. Brinsley, P. N. Salkeld, and C. H. Lucas. 2000. Influence of biota on spatial and temporal variation in sediment erodability and material flux on a tidal flat (Westerschelde, The Netherlands). Mar. Ecol. Prog. Ser. **194**: 23–37.

Widdows, J., P. L. Friend, A. J. Bale, M. D. Brinsley, N. D. Pope, and C. E. L. Thompson. 2007. Inter-comparison between five devices for determining erodability of intertidal sediments. Cont. Shelf Res. **27**: 1174–1189.

Widdows, J., N. D. Pope, M. D. Brinsley, H. Asmus, and R. M. Asmus. 2008. Effects of seagrass beds (*Zostera noltii* and *Z. marina*) on near-bed hydrodynamics and sediment resuspension. Mar. Ecol. Prog. Ser. **358**: 125–136.

Willows, R. I., J. Widdows, and R. G. Wood. 1998. Influence of an infaunal bivalve on the erosion of an intertidal cohesive sediment: A flume and modeling study. Limnol. Oceanogr. **43**: 1332–1343.

Wootton, J. T. 2002. Indirect effects in complex ecosystems: Recent progress and future challenges. J Sea Res **48**: 157–172.

Wright, L. D., J. D. Boon, J. P. Xu, and S. C. Kim. 1992. The bottom boundary layer of the bay Stem Plains environment of lower Chesapeake Bay. Est. Coast. Shelf Sci. **35**: 17–36.

Xia, X., and others. 2017*a*. Enhanced nitrogen loss from rivers through coupled nitrification-denitrification caused by suspended sediment. Sci. Total Environ. **579**: 47–59.

Xia, X., Z. Jia, T. Liu, S. Zhang, and L. Zhang. 2017*b*. Coupled nitrification-denitrification caused by suspended sediment (SPS) in rivers: Importance of SPS size and composition. Environ. Sci. Technol. **51**: 212–221.

Yamamoto, Y. 2010. Contribution of bioturbation by the red swamp crayfish *Procambarus clarkii* to the recruitment of bloom-forming cyanobacteria from sediment. J. Limnol. **69**: 102–111.

Zhang, Q., D. C. Brady, and W. P. Ball. 2013. Long-term seasonal trends of nitrogen, phosphorus, and suspended sediment load from the non-tidal Susquehanna River basin to Chesapeake Bay. Sci. Total Environ. **452–453**: 208–221.

Zhou, Q., L. Li, L. Huang, L. Guo, and L. Song. 2018. Combining hydrogen peroxide addition with sunlight regulation to control algal blooms. Environ. Sci. Pollut. Res. Int. **25**: 2239–2247.

Zhu, X., G. Dao, Y. Tao, X. Zhan, and H. Hu. 2021. A review on control of harmful algal blooms by plant-derived allelochemicals. J. Hazard. Mater. **401**: 123403.

Conflicts of Interest

ETP and JCC have no conflicts of interest.